Electrochemical Passivation of 316L Stainless Steel for Biomedical Applications: A Method for Improving Pitting Corrosion Resistance via Cyclic Potentiodynamic Polarization

---

by

Kang Hoon Choi

McGill University, Montreal

Department of Chemical Engineering

April 2019

A thesis submitted to McGill University in partial fulfillment of the requirements of the degree of Master of Engineering

ABSTRACT

316L stainless steels (SS) are widely used as biomaterials due to their good general corrosion resistance, low cost and good machinability. However, 316L SS is prone to severe degradation in human body due to aggressive halide ions present in the environment, namely chlorides and bromides, which can cause a local breakdown of the protective passive film and enable the progression of pitting corrosion. Hence, significant efforts have been made to develop methods for the surface modification of the 316L SS in order to improve its pitting corrosion resistance, and thus its biocompatibility.

In this work, the application of cyclic potentiodynamic polarization (CPP) for the formation of a highly corrosion resistant passive oxide film on a 316L SS surface using a 0.1 M $NaNO_3$ solution as a passivation electrolyte in deaerated and aerated conditions was investigated. Electrochemical tests such as open circuit potential (OCP) measurement and potentiodynamic polarization test were conducted to evaluate the corrosion behavior of the modified surface. It was found that CPP method under both deaerated and aerated conditions resulted in formation of a passive oxide film that offers significantly higher OCP and pitting corrosion resistance than the naturally-grown passive film. The results of OCP and potentiodynamic polarization tests show that the passive film formed by CPP in an aerated 0.1 M $NaNO_3$ solution exhibits higher OCP and higher pitting corrosion resistance than the film formed in a deaerated 0.1 M $NaNO_3$ solution. It was observed that dissolved oxygen has a positive effect on the passivation of 316L SS under CPP conditions. The 316L SS surface passivated for 200 sweeps in an aerated 0.1 M $NaNO_3$ solution exhibited largest improvements: highest open circuit potential (141.77 mV_{SCE}) and complete elimination of pitting corrosion in a 0.1 M PBS solution at 22 °C.

RÉSUMÉ

Les aciers inoxydables 316L sont utilisés partout comme biomatériaux en raison de leur bonne résistance à la corrosion, de leur faible coût et de leur bonne usinabilité. Cependant, lorsequ'ils sont utilises dans le corps humain, les aciers inoxydables 316L se dégradent à cause de la présence d'ions halogénures agressifs. En particulier, les chlorures et les bromures peuvent provoquer une dégradation locale du film protecteur passif et permettre la progression de la corrosion par piqûre. Par conséquent, des recherches sont en cours pour développer des méthodes de modification de surface de l'acier inoxydable 316L afin d'améliorer sa résistance à la corrosion par piqûre et donc sa biocompatibilité.

Dans ce travail, l'application de la polarisation potentiodynamique cyclique pour la formation d'un film d'oxyde passif résistant à la corrosion sur une surface en acier inoxydable 316L a été étudiée. Ceci a été fait en utilisant une solution de $NaNO_3$ 0.1 M pour l'électrolyte de passivation dans des conditions désaérées et aérées. Des tests électrochimiques étaient faits pour évaluer le comportement à la corrosion de la surface modifiée. Cela incluait des mesures de potentiel en circuit ouvert et un test de polarisation potentiodynamique. Il a été constaté que la méthode de polarisation potentiodynamique cyclique dans les deux conditions entraînait la formation d'un film d'oxyde passif présentant un potentiel de circuit ouvert et une résistance à la corrosion par piqûres nettement supérieurs à ceux du film passif développé naturellement. Il a été constaté que la méthode de polarisation potentiodynamique cyclique dans les deux conditions entraînait la formation d'un film d'oxyde passif possédant un potentiel de circuit ouvert et une résistance à la corrosion par piqûres significativement supérieurs à ceux du film passif développé naturellement. En outre, les résultats des tests de potentiel de circuit ouvert et de polarisation potentiodynamique montrent que le film passif formé par polarisation potentiodynamique cyclique dans une solution aérée de $NaNO_3$ 0.1 M présente un potentiel de circuit ouvert et une résistance à la corrosion par piqûre supérieurs à ceux du film formé dans une solution de $NaNO_3$ 0.1 M desaérée. Il a été observé que l'oxygène dissous avait un effet positif sur la passivation de l'acier inoxydable 316L dans des conditions de polarisation potentiodynamique cyclique. La

surface en acier inoxydable 316L passivée pendant 200 balayages dans une solution aérée de $NaNO_3$ 0,1 M présentait les améliorations les plus importantes: potentiel de circuit ouvert maximum (141,77 mV_{SCE}) et élimination complète de la corrosion par piqûre dans une solution de PBS 0.1 M à 22°C.

ACKNOWLEDGEMENTS

Firstly, I would like to thank my family for their unconditional love and support. I would not have been able to complete my thesis without the encouragements and support from them. Thank you for being my inspiration and my strength. I want to thank my fiancée, Jie Soo, for supporting me and making me smile through stressful times. I am grateful to have you by my side.

I would like to express my sincerest gratitude and appreciation to my thesis supervisor Prof. Sasha Omanovic for his generosity, kindness and continuous support. I would not have been able to overcome numerous obstacles that came up throughout the period of this project without his support and help.

A special thank you goes to Prof. In-Ho Jung at Seoul National University for his continuous support over the years and advices on pursuing graduate studies in the field of corrosion science.

I gratefully acknowledge Prof. Anne-Marie Kietzig for reviewing my thesis and for her valuable input and recommendations as an external examiner.

I would like to thank my former and current colleagues in the Electrochemistry and Corrosion Lab: Mario, Saloumeh, Abraham, Emmanuel, Elmira, Deepak, Mahmoud, Aqeel, Ahmad, Amir, Logan, Xingge, Rihab, Zhuoya, and Hao for the stimulating discussions, for the sleepless nights we were working together. A special thank you goes to Elmira for her assistance in helping me with my experimental setup and also the preparation of my samples. I would like to thank Mr. Frank Caporuscio, Mr. Ranjan Roy, and Mr. Andrew Golsztajn for all the help they provided during my research.

Finally, I would like to acknowledge the financial support from the Eugenie Ulmer-Lamothe Foundation and the Department of Chemical Engineering.

TABLE OF CONTENTS

LIST OF FIGURES

LIST OF TABLES

CHAPTER 1: INTRODUCTION

The demand for biomaterials is increasing rapidly with the growing population of elderly people who have a higher risk of failed tissue. Significant developments have been taking place to provide suitable biomaterials to replace diseased or damaged parts in the human body in order to improve or restore tissue function, thereby improving the quality of life. With the advancement in manufacturing of biomaterials, all classes of materials including metal, ceramic, polymer and composite have drawn attention in biomedical applications. Among these materials, metallic biomaterials have played a predominant role as they have been successfully used in clinical applications such as in orthopedic, oral and maxillofacial, cardiovascular, and surgical instruments [1]. The three most commonly used metallic biomaterials are 316L stainless steel, cobalt-chromium alloy, and titanium and its alloys. Among these metals, titanium alloys exhibit the highest biocompatibility, corrosion resistance, and specific strength, but they are the most expensive materials compared with 316L stainless steel and cobalt-chromium alloys [2]. Unfortunately, relatively few metals in industrial use are biocompatible and sufficiently corrosion resistant for long-term use as an implant in human body [1].

316L stainless steel (SS) is among the most widely used types of implant material and has the longest record of practical use due to its high corrosion resistance, low cost, appropriate mechanical properties, and good machinability [3]. Its excellent resistance to uniform corrosion is related to the passive oxide film on its surface. However, recent decades of clinical trials and studies have shown that 316L SS is prone to severe degradation in human body due to aggressive halide ions present in the environment, namely chlorides and bromides, which can cause a local breakdown of the protective passive film and enable the progression of pitting corrosion [1]. Pitting corrosion has detrimental effects on metallic surgical implants since it adversely affects both biocompatibility and mechanical strength of the implant. Pitting corrosion is a form of highly localized corrosion that leads to formation of small cavities on the surface of protective passive film, and subsequently leads to release of metal ions into the surrounding environment. This is concerning when using 316L SS as a biomedical implant because the release of harmful products, especially nickel and chromium ions, into the human body may cause detrimental biological reactions [4,5]. Consequently, its main applications are limited to medical surgical instruments, implant manufacturing processes, and short-term implant devices [2]. Therefore, it

is of practical interest to enhance the corrosion resistance, especially pitting corrosion resistance, of 316L SS by employing suitable surface treatment methods.

The relatively good general corrosion resistance of stainless steels results from its ability to spontaneously form a stable self-healing chromium-rich oxide film, a so-called passive oxide film, on its surface in the reaction with oxygen from air or most aqueous environment [6]. This passive film acts as a barrier protecting the metal surface from the corrosive environment. It has been well-investigated that the semiconductivity of a passive oxide film can be either *n*-type or *p*-type, which is dependent on the predominant charge carrier density present in the oxide layer [7]. Extensive research on the capacitance measurements of austenitic stainless steels have revealed that the *n*-type semiconducting properties are associated with the outer iron oxide part of the passive film, which are characterized by the presence of oxygen vacancies in the film, whereas the *p*-type semiconducting properties are correlated with the inner chromium oxide region, which are characterized by a deficiency in metal ions or with excess of cation vacancies [7,8]. *n*-type passive layers are susceptible to pitting corrosion because of their high density of oxygen vacancies which act as pitting initiation sites that allow the penetration of aggressive halide anions through the passive film. Contrarily, *p*-type passive layers have excellent pitting resistance because of their high density of cation vacancies which inhibit penetration of aggressive halide anions into the film. Hence, the present work aims to improve the pitting corrosion resistance of 316L SS by possibly transforming the semiconducting property of the outer oxide layer from *n*-type to *p*-type, thereby reducing the susceptibility to the aggressive anionic penetration.

The surface property of the passive oxide film is the most important factor that determines the corrosion behaviour of stainless steels. As mentioned earlier, although 316L SS has excellent bulk mechanical and physical properties, its poor localized corrosion resistance has limited its applications as biomedical implants. Hence, numerous studies have been carried out on the surface modification of 316L SS in order to selectively achieve desirable surface properties while preserving the valuable properties of the bulk material [9]. Various types of surface modification techniques have been reported such as ion implantation [10–12], bioactive

ceramic coatings [13–16], electropolishing [17–19] and cyclic potentiodynamic polarization [20–24]. In particular, the surface modification by cyclic potentiodynamic polarization (CPP) is a very effective passivation technique that can enhance the pitting corrosion resistance of 316L SS. This technique enhances the passive properties of oxide films by exploiting the kinetics of the redox reactions that occur in response to the surrounding environment since passive film formation is highly dependent on the type of solution or atmosphere used. In fact, this technique has been successfully applied in our lab to produce highly-protective passive oxide films on 316LVM stainless steel by using a deaerated 0.1 M $NaNO_3$ solution as the passivation electrolyte [21,22] (it should be noted that the "LVM" type of 316 stainless steel has a lower content of carbon and impurities than the "L" type used in this work, the latter being, thus, more prone to corrosion than the LVM type). Hence, the present research aims to contribute towards further development of CPP technique by incorporating dissolved oxygen into the passivation electrolyte. The rationale for the incorporation of dissolved oxygen in the passivating solution is based on its two different roles on the passivation phenomenon claimed by several studies: (i) it acts as a cathodic depolarizer, which facilitates the kinetics of both anodic and cathodic passivation processes by reacting with the hydrogen gas surrounding the cathode and thereby speeding up the passivation process [25,26], and (ii) it acts as a passivating agent by providing necessary chemical species for passivation [27,28]. However, despite many reports, the effects of dissolved oxygen on the passivation mechanism are inconsistent and depend on the electrochemical systems involved in the types of materials and solutions. Also, there has not been a CPP technique that utilizes dissolved oxygen to improve the passive properties of stainless steels. Hence, the present research aims to investigate the influence of dissolved oxygen on passivation by comparing the corrosion behaviours of the passive film formed in absence and in presence of dissolved oxygen.

The main goal of the present research is to develop and optimize a simple electrochemical cyclic potentiodynamic polarization for the formation of highly corrosion resistant passive oxide film on 316L SS using 0.1 M $NaNO_3$ solution in deaerated and aerated conditions. The influences of number of polarization scans and dissolved oxygen on the resulting corrosion behaviour were investigated with the aim of achieving high resistance to both general

and pitting corrosion in a physiological simulating solution (phosphate buffer saline solution pH 7.4, 0.027 M KCl and 0.137 M NaCl). Hence, the present work is ultimately aimed at contributing to the development of more biocompatible 316L stainless steel based implants.

CHAPTER 2: BACKGROUND AND LITERATURE REVIEW

2.1 Type AISI 316L Stainless Steel

Type AISI 316L stainless steel (SS), a single phase austenitic stainless steel, is one of the most commonly used materials for biomedical implant applications due to its relatively low cost, ease of fabrication, moderate strength, and reasonable corrosion resistance. The "L" in 316L designates low carbon content (<0.03%) in the alloy [3]. Low level of carbon content in the alloy is necessary to prevent formation of chromium carbides since these carbides can form preferentially along grain boundaries, leaving the adjacent areas with depleted chromium levels which are thus prone to intergranular corrosion [3]. Chromium is present in 316L SS passive oxide film primarily in the form of a Cr_2O_3 surface layer, which is crucial to its corrosion resistance. This surface layer is known as the passive oxide film, which is highly adhesive and promotes self-healing in the presence of oxygen. The minimum percentage of chromium in stainless steels is about 11 wt.%, which is known as the minimum amount required to prevent the formation of rust in an unpolluted atmosphere [1]. Further enhancement in corrosion resistance, as well as mechanical properties, is achieved by the presence of other alloying elements. The presence of nickel, molybdenum and nitrogen in 316L SS stabilizes the formation of an austenite phase and also contributes to its increased corrosion resistance [1,3]. Alloying elements such as chromium and nickel provide oxidation resistance while molybdenum and nitrogen enhance the localized corrosion resistance of 316L SS [1,3]. Molybdenum is considered as one of the principal alloying elements in austenitic stainless steel which enhances the pitting corrosion resistance by molybdenum carbide formation, thereby reducing the amount of chromium carbide formation [1,3]. Nickel is the main alloying element that stabilizes the formation of austenite in stainless steel and also contributes to increased corrosion resistance by the formation of protective oxide films [1,3]. Nevertheless, 316L SS implants experience electrochemical dissolution in the human body environment, which consists of an ample amount of corrosive minerals such as chlorides, amino acids and proteins [29]. In fact, 90% of the failure of 316L SS implants are due to localized corrosions such as pitting and crevice corrosions [30]. Furthermore, the corrosion of a 316L SS implant gives adverse effects to the surrounding tissues since nickel and chromium ions are highly toxic to the human body [31].

316L SS is an excellent example of an alloy that exhibits corrosion resistance in a variety of environments as a result of surface passivation. Thus, 316L SS is extensively employed in various industrial applications such as architectural structures, automotive parts, and biomedical devices [1]. In biomedical applications, 316L SS comprises a substantial percentage of clinical use as it is currently used in orthopedic surgery as temporary fixation devices (nails, screws, plates, and wire) [32], cardiovascular surgery (e.g., electric terminal and stents) [33], and surgical instruments (e.g., bone drills, knives, needles, etc.) [1]. Despite these applications, the resistivity of 316L SS to pitting corrosion is still not satisfactory for long-term applications. Therefore, its current applications are mostly confined to short-term implant devices, medical surgery instruments, and implant manufacturing equipment; nevertheless, 316L SS is still the predominant material used for coronary stents, which are long-term implants [2].

While 316L SS is one of the oldest and most common alloys in use, more recent developments have led to stainless steels with enhanced corrosion resistance and mechanical properties. Advanced steel-making processes such as vacuum melting, vacuum arc re-melting (VAR) or electro-slag refining are used to produce highly corrosion resistant stainless steel grades [1]. These production methods are employed to produce cleaner varieties of stainless steels in order to minimize the traces of undesirable elements such as sulfur and phosphorous in the alloy, thereby avoiding the unwanted formation of secondary phases and inclusions especially at grain boundaries. For example, the vacuum melting process is used to produce 316LVM stainless steels which has improved resistance to pitting corrosion due to its relatively low sulfur content compared to 316L SS. Despite the aforementioned production techniques, 316L is still the most employed metallic biomaterial due to its low production cost. As discussed previously, enhancement in corrosion resistance of 316L SS is an undeniable requirement to maintain and extend its usage in implant applications.

2.2 Passive Oxide Film

As mentioned above, good corrosion resistance of 316L SS is due to the presence of a self-healing protective passive oxide film on its surface. Although the thickness of the passive oxide film is typically only a few nanometers, it acts as a highly protective barrier between the bulk of the metal substrate and the aggressive biological environment. Depending on the type of oxide formed, the passive film may or may not be stable upon exposure to the biological environment. In fact, a variety of factors can influence the stability of the passive film against dissolution, which include the film's chemical composition, structure, surface morphology, semiconducting/electronic properties, mass-transport properties, and breakdown of passivity in the biological environment. The following sections will address theoretical aspects and elaborate on each of these properties.

2.2.1 Structure

Several studies have demonstrated the dependence of the passive film structure on the corrosion resistance of stainless steel [34,35]. One of the earliest investigations on the crystal structure of passive films on iron-chromium alloys was carried out by McBee and Kruger [36] in 1972 using transmission electron-diffraction microscopy at 100 kV. The diffraction patterns obtained revealed that the passive oxide films on the highest chromium-content alloy, Fe-24%Cr alloy were amorphous, whereas 0-10%Cr in the bulk resulted in a spinel-like structure. They reported that the films tend to become amorphous as the chromium content of the alloy is increased. Ryan et al. [37,38] investigated iron-chromium alloys in sulfuric acid solution and iron in borate buffer solution and confirmed the conclusion made from McBee and Kruger [36] that the passive film is amorphous for chromium concentrations above 12-19%. In another study, Marcus [39] examined the atomic structure of passive films on stainless steel alloys by performing scanning tunneling microscopy and characterized the influence of structural modifications occurring in the passive film during polarization at a potential in the passive region. His first finding was that after 2 hours of polarization, the film was disordered. After

prolonged polarization (63 hours), growth of the crystallized regions was found in the film structure, and the resulting electrochemical measurements showed that the crystallized film was more stable during exposure to air than the disordered film.

2.2.2 Thickness of Passive Oxide Film on 316L Stainless Steel

The influence of the thickness of passive film on austenitic stainless steel has been examined in numerous studies [40–42]. For example, Xu et al. [41] investigated the passive film growth on 316L SS in borate buffer solution using real-time spectroscopic ellipsometry, and concluded that the thickness of potentiostatically-polarized passive film increased linearly with applied potential. A similar potential dependence of surface film thickness on 304 stainless steel during potentiodynamic polarization was found by Olsson and Landolt [42]. Shahryari et al. [22] studied a passive film formed on 316LVM stainless steel by cyclic potentiodynamic polarization and demonstrated that CPP induces significant changes in the structure of the passive film. Comparison of their TEM images observed on unmodified and CPP-modified passive films with their electrochemical measurements results revealed that the CPP-modified passive film is significantly thicker and exhibits higher corrosion resistance. On the other hand, Shih et al. [35] studied the effect of different passivation processes on the corrosion resistance of 316L SS. They showed that the removal of a naturally-formed oxide layer and the replacement by a more uniform and compact surface oxide layer, rather than its thickness, is the predominant factor influencing the corrosion behavior of stainless steel. Furthermore, they concluded that the improvement in the corrosion resistance of 316L SS was attributed to the modified compositional properties of these newly grown passive films, which are composed of nano-scale oxide particles with higher oxygen and chromium concentrations [35].

2.2.3 Chemical Composition of Passive Oxide Film on 316L Stainless Steel

The corrosion behavior of stainless steel is strongly influenced by the chemical composition of its surface oxide layer. The chemical composition and elemental depth profiles of the passive oxide film on 316L SS have been extensively studied through the analysis by Auger electron spectroscopy (AES) and X-Ray photoelectron spectroscopy (XPS) [8,35,43,44]. It has been well-documented that the passive oxide film has a duplex structure which consists of an inner region composed of a chromium-rich oxide layer in contact with the metallic substrate, whereas the outermost layer is comprised of iron-rich oxides and hydroxides. Figure 2-1 shows an example of the Auger depth composition profiles of passive films formed on 304 and 316 stainless steels obtained from the AES analysis by Hakiki et al. [8]. As it can be observed from both passive films, the inner region of the passive film is enriched in chromium oxide close to the alloy, whereas the outer region of the passive film is depleted in chromium and comprised mainly of iron oxide. Also, a small amount of nickel oxide is detected in the iron oxide region, which suggests the existence of mixed iron-nickel oxides. Although molybdenum is not detected by this AES analysis, molybdenum is present in the passive film but in negligible amount [35]. In fact, molybdenum as an alloying element modifies the iron depth profile in the passive film [8]. As it can be seen in Figure 2-1, the passive film formed on the 316 SS has a much higher Mo content, a much lower atomic density of iron oxide, and higher overall atomic density than the 304 stainless steel. In another study by Lorang et al. [43], observations of the concentration profile indicate that the thickness of the passive film formed on 304 stainless steel increases both with the applied passivation potential and with the temperature. However, it was found that the thickness of the innermost (chromium-rich oxide) region is only dependent on the applied potential but is not much influenced by the temperature [43]. Based on the results of AES and XPS obtained by Lorang et al. [43], it was determined that the composition of bulk oxide in the innermost layer of the passive film existed in the form of Cr_2O_3, whereas various forms of iron oxides (Fe_3O_4, Fe_2O_3, $Fe(OH)_2$, and FeOOH) were observed in the outer region of the film. Numerous studies on the effects of these compounds on the corrosion resistance of stainless steels have been reported, and it was found that chromium-rich oxide layers are mainly responsible for the high passivation ability of these alloys [1,22,35,40,45]. Moreover, chromium

enrichment in the passive film achieves its high corrosion resistance due to the change in the semiconducting/electronic structure of passive film, which will be discussed in detail in the subsequent section.

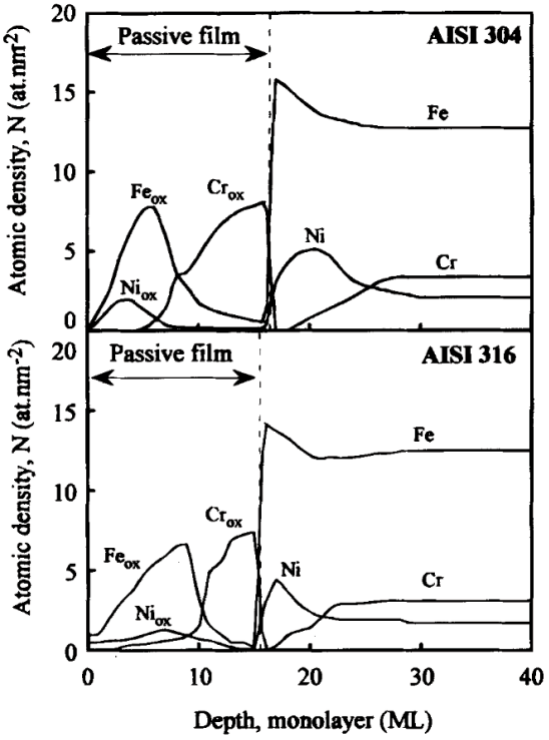

Figure 2-1 Auger depth concentration profiles of passive films formed on 304 and 316 stainless steels [8].

2.2.4 Semiconducting Properties of the Passive Film

One of the principal factors thought to control the corrosion behavior of a passive film formed on stainless steel is its semiconducting/electronic properties. In order to understand the correlation between the corrosion resistance and semiconducting properties of the passive films, extensive research has been conducted using capacitance measurements to determine these properties through the Mott-Schottky approach [21,22,46–48]. As discussed in the previously section, the AES and XPS analyses show that the passive films formed on the surface of

austenitic stainless steels have a bi-layer structure, which is comprised of chromium-rich oxide in the inner region and an external layer of iron oxides [8]. These passive oxide layers are known to exhibit semiconducting properties either as *n*-type or *p*-type, which are determined by the predominant defect in the oxide layer [7,8,49]. The capacitance measurements have revealed that the *n*-type semiconducting properties are associated with the outer iron oxide part of the passive film, which are characterized by the presence of oxygen vacancies in the film [7,8]. This external layer of iron oxides in the passive film of stainless steel is known to exhibit poor pitting resistance since its higher density of oxygen vacancies act as pitting initiation sites [22]. On the other hand, *p*-type semiconducting properties are correlated with the inner chromium oxide region, which are characterized by a deficiency in metal ions or excess with cation vacancies [7,8].

The Mott-Schottky approach is a common method used to determine type of semiconductivity of 316L SS surface in the potential region where pitting occurs. Shahryari et al. [22] examined the semiconducting behavior of a naturally-formed passive film on 316LVM stainless steel and the passive films modified by cyclic potentiodynamic polarization using Mott–Schottky approach and determined the type of semiconductivity by characterizing the existence of multiple potential regions. In the pitting susceptible potential region, it was found that the unmodified surface has a positive slope, which indicates it as an *n*-type semiconductor, whereas the passive film modified by CPP has a negative slope, indicating its semiconducting behavior as a *p*-type. Hence, using the Mott-Schottky approach, Shahryari et al. [22] reported that CPP is an effective surface modification method for transforming the semiconductivity of the passive film on 316LVM stainless steel from *n*-type to the *p*-type.

2.2.5 Migration of Ions in Passive Oxide Film

The importance of the type and the concentration of cation and anion defects present in a passive oxide film was discussed in the previous section through Mott-Schottky analysis. The transport of these point defects or ions and their interfacial reactions through the passive film

ultimately determine the passivity and breakdown of the film. The phenomenon of passivation on a metallic surface was first discovered by Keir in 1790 [50], who observed the absence of dissolution for iron immersed in concentrated nitric acid compared to high rate of dissolution when immersed in dilute nitric acid. Since then, a class of models is available that investigate the growth kinetics and breakdown of passivation on metallic surfaces [46,51–53]. As discussed in the previous section, the passive oxide film on a stainless steel surface is characterized by a bipolar structure, consisting of cation vacancies in the inner layer, i.e. *p*-type semiconductivity, and anion vacancies in the outer layer, i.e. *n*-type semiconductivity [8,47]. As a result, the passive film is characterized by selective-ion permeability. In general, the film growth proceeds by oxygen ions migrating toward the metal/oxide interface through anion vacancies which react with metal ions to form an inner part of the oxide film, while metal ions migrate toward the oxide/electrolyte interface through cation vacancies and react with oxygen ions and other anions present in the electrolyte to form an outer part of the oxide film [54]. Consequently, this type of bipolar ion-selective oxide film blocks the ion transport across the structure of the passive film and enhances the general corrosion resistivity. However, in the presence of aggressive anionic species (e.g. chloride anions), the outermost *n*-type oxide layer is highly susceptible to local breakdown of the film eventually leading to the dissolution of the metal substrate at the site of localized breakdown, which is known as the pitting corrosion [54]. Hence, the present research aims to enhance the resistivity of 316L SS to pitting corrosion by transforming the semiconductivity of the outer oxide layer from *n*-type to *p*-type.

2.3 Corrosion of Metallic Implant

Corrosion is the destruction or deterioration of a metallic material due to its reaction with its surrounding environment [1]. Simply, corrosion is the desire of metals to return to their natural form. This is because metals in contact with oxygen-containing atmospheres, practically all environments including the human body, are fundamentally unstable. The relevant form of corrosion related to metallic biomaterials is the aqueous or electrochemical corrosion. In general,

there are two reactions that occur in an electrochemical corrosion reaction: the anodic reaction, in which metallic implant is oxidized to its ionic form:

$$M \rightarrow M^{n+} + ne^{-} \qquad \text{Equation 2-1}$$

and the cathodic reaction, in which the electrons so generated are consumed in the reduction of hydrogen (if there is no oxygen present in the electrolyte):

$$2H^{+} + 2e^{-} \rightarrow H_2 \qquad \text{Equation 2-2}$$

or in the reduction of dissolved oxygen, in acidic solutions:

$$O_2 + 4H^{+} + 4e^{-} \rightarrow 2H_2O \qquad \text{Equation 2-3}$$

or in neutral or basic solutions [3]:

$$O_2 + 2H_2O + 4e^{-} \rightarrow 4OH^{-} \qquad \text{Equation 2-4}$$

In all cases, the basic principle of electrochemically-based metallic corrosion is that the rate of the anodic or oxidation reaction must equal the rate of the cathodic or reduction reaction [3]. In other words, the corrosion reaction will occur transiently and effectively stop when equilibrium is reached between the anodic and cathodic reaction. However, this only occurs in conditions where a homogeneous pure metal exists within an unchanging environment, which is highly unrealistic especially in a biological environment. In reality, as a corrosion reaction takes place, the relative movement of involved ions will continuously modify the composition of the surrounding environment and the surface of the involved metal. Hence, this dynamic nature will result in continued reaction, namely a sustained corrosion reaction, between the metal surface and the surrounding environment to attempt to establish an equilibrium. The extent to which the corrosion reaction proceeds depends on the system of the metallic material and the surrounding environment since different conditions can result in different overall corrosion rate by influencing either the anodic or cathodic reactions. Hence, the same concept can be applied in developing highly corrosion-resistant metallic biomaterials by obstructing either the anodic or

cathodic reactions in order to stop the corrosion process. However, as evidenced by many cases of metallic implant failures, corrosion is a major problem for using metallic biomaterials as implant devices due to the complex constituents of physiological environment. In fact, 90% of the failure of 316L SS implants are due to localized corrosions, especially pitting corrosions [29]. Furthermore, the corrosion of 316L SS implant has detrimental effects on the surrounding tissues and the implant itself since harmful metallic ions, especially nickel and chromium ions, can accumulate in the human body and the mechanical integrity of the implant can also be deteriorated. In particular, the release of nickel and chromium ions to the surrounding tissues is serious problem as they can cause detrimental biological reactions [5,6]. Studies have shown that nickel ions may cause cutaneous inflammations and chromium ions may cause ulcers and central nervous system disturbances, and both products may also lead to carcinogenicity in the human body [55–57]. Consequently, the effects of these potentially toxic ions limit the use of 316L SS implants to temporary or short-term applications.

2.3.1 The Human Body as a Corrosive Environment

Localized breakdown of passive films becomes a greater concern when a metallic implant is placed in the hostile electrolytic environment of a human body. Under normal conditions, the human body is a highly corrosive environment due to the constituents of physiological fluid which include various anions, cations, organic substances, and dissolved oxygen [29]. The anions are mainly chloride, phosphate, and bicarbonate ions [3]. The principal cations are Na^+, K^+, Ca^{2+}, and Mg^{2+}, plus smaller amounts of many other cations [3]. Table 2-1 gives the range for the anion and cation concentrations in blood plasma and extracellular fluid [58]. The presence of these complex physiological constituents can interfere with the equilibrium between the implant surface and the surrounding environment, which will lead to continued corrosion of the implant. Furthermore, once metal ions are released into the body, the pH value of body fluid may fall to 3-4, which presents an even more corrosive environment for metallic implants [59]. In addition, the internal partial pressure of oxygen in human body, approximately one quarter of

atmospheric oxygen pressure, creates a condition that hinders the repassivation of the depassivated areas on the surface films [3]. As a result, preferential corrosion of the oxygen-deficient regions can occur, which will lead to the localized breakdown of the passive film. Thus, a metal that may be inert or passive in atmospheric conditions may undergo corrosion in the human body.

Table 2-1 Ionic Concentrations in Blood Plasma and Extracellular Fluid [58].

Anion, Cation	Blood Plasma (m*M*)	Extracellular Fluid (m*M*)
Cl^-	96-111	112-120
HCO_3^-	16-31	25.3-29.7
HPO_4^{2-}	1-1.5	1.02-1.93
SO_4^{2-}	0.35-1	0.4
$H_2PO_4^-$	2	-
Na^+	131-155	141-150
Mg^{2+}	0.7-1.9	1.3
Ca^{2+}	1.9-3	1.4-1.55
K^+	3.5-5.6	3.5-4

2.4 Pitting Corrosion

Although 316L SS are widely used in biomedical applications because of their good general corrosion resistance, they are nevertheless susceptible to localized types of corrosion. This is evidently true in the human body, which is a highly corrosive environment due to hostile electrolytic constituents present in the body fluid. In fact, pitting corrosion is one of the most common and catastrophic causes of failure of 316L SS implants as it often proceeds undetected with very little metal loss until fracture occurs. Pitting corrosion is a form of highly localized corrosion that leads to the formation of small cavities on the surface of protective passive film, and subsequently leads to the release of metal ions to the surrounding environment [60]. The initiation and breakdown of passivity are shown in Figure 2-2. In general, the formation of such pits is due to the interaction of aggressive ions with the oxide film at areas where it is defective

or weak in nature. Also, studies have shown that pitting corrosion occurs more frequently in media containing halide ions, especially chloride ions [61]. Pitting typically initiates from a localized surface defect such as a scratch or a slight variation in composition (i.e. alloy heterogeneities in the surface layer) that become anodic while the remaining vast area outside the pit becomes cathodic [62]. This results in a difference in electrochemical potential between the base of the pit and the surrounding metal, releasing metal ions that may form oxides at the top of the pit, thereby renewing the passivation. Once pitting initiates on a surface, it becomes an autocatalytic reaction due to differential aeration conditions between the inside of the tip and the flat surface of the metal, which causes the pitting attack to propagate through the metallic bulk until it leads to the complete breakdown of passivity.

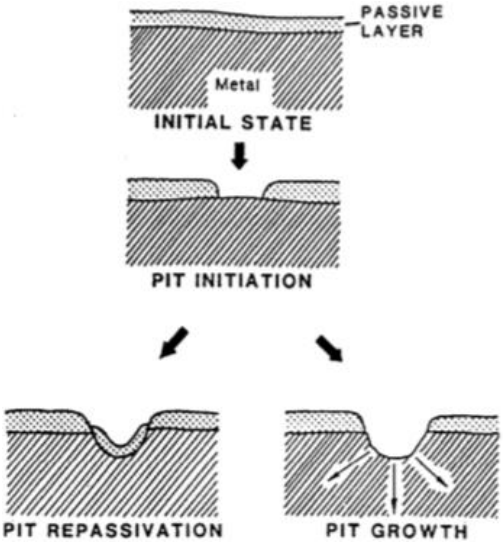

Figure 2-2 Stages of pitting corrosion [60].

A number of theoretical models have been proposed to describe pitting initiation processes leading to passive film breakdown, and they have been categorized into three main mechanisms focused on passive film penetration, film breaking, and adsorption [63]. The penetration mechanism, first discussed by Hoar et al. [64], involves the transfer of aggressive anions through the passive oxide film to the metal surface, where they start localized dissolution of the surface. In this theory, the migration of anions is explained by the high electric field

strength in the passive oxide film and also a high defect concentration within the presumably disordered structure of the oxide film [64]. The penetration of aggressive anions in the film further increases the ionic conductivities along the penetration paths. Hence, the pitting penetration becomes an autocatalytic process, which undermines the passive film structure by vacancy formation and condensation at the metal/film interface, or rapid cation release at the film/electrolyte interface. Based on these concepts of penetration mechanism, Macdonald et al. [65–67], developed a well-known theory called the point defect model (PDM), which describes the growth and the passivity breakdown through the transport of point defects, i.e. electrons, holes, and metal and oxide vacancies, across the passive film. PDM assumes that adsorption of chloride ions and its incorporation at the outer surface of the oxide film results in the formation of cationic vacancies [66]. These cation vacancies migrate to the metal/film interface where they are compensated by the transport of cations from the metal in the opposite direction through oxidation. If this flux of vacancies through the oxide film is at a higher rate than the oxidative injection of cations from the metal, cation vacancies may accumulate and form voids at the metal/film interface. When the voids grow to a critical size, the passive film will collapse and subsequently lead to pit growth.

The film-breaking mechanism, proposed by Sato et al. [68,69], requires the occurrence of fissures within the passive film that give direct access of anions to the unprotected metal surface. Another explanation on the film-breaking mechanism, reported by Haupt and Strehblow [70], was that chemical changes, i.e. a reduction of Fe(III) to Fe(II), by a sudden change of the electrode potential can cause stresses within the film, and hence the breakdown of oxides.

The adsorption mechanism, first discussed by Kolotyrkin [71] and Hoar and Jacob [72], begins with localized adsorption of aggressive anions at the oxide/electrolyte interface, which catalytically enhances the oxide dissolution at these sites. As a result, this causes the thinning of the passive film until a complete removal is achieved and eventually leads to pit growth. Although an extensive array of theoretical models for the pitting mechanism have been proposed, the prediction of pitting initiation remains difficult due to its dynamic nature, which depends on the type of passive oxide film and its surrounding environment.

2.4.1 Pitting Polarization Measurement

A typical potentiodynamic polarization curve for stainless steel in the presence of oxygen is exemplified in Figure 2-3. Potentiodynamic polarization is a useful technique for determining the kinetics of the different stages of the corrosion process, especially for characterizing the susceptibility of a metal or alloy to pitting corrosion. As illustrated in Figure 2-3, a polarization curve for a passive metal can be divided into three regions, namely active, passive, and transpassive. In the active region, the anodic and cathodic processes are in equilibrium, which results in a large drop in net current value [73]. This value is known as the corrosion potential, E_{corr}, or sometimes called the open circuit potential, OCP. As the anodic polarization scan advances to the passive region, the passive film becomes stable and retains its passivity up to the pitting potential. This passive state can be quantitatively characterized by the passivation current density, j_{pass}, which is the minimum current density required to maintain the thickness of the film in the passive range [73]. Once pitting initiates at the pitting potential, the passive film enters the transpassive region where a pitting attack propagates rapidly, as shown in Figure 2-3 by the sharp rise in current density with electrode potentials just above the pitting potential. The pitting potential, E_P, is a well-defined electrode potential that indicates the initiation of pitting corrosion for a given metal or alloy [73]. The pitting potential depends on several factors such as the concentration of halide ions, the surface properties of the material, and temperature [60,73]. Hence, the pitting potential of different materials is only comparable if the above-mentioned factors are kept the same in the experimental conditions. For given experimental conditions, a more positive pitting potential value indicates a higher resistance against pitting corrosion. On the other hand, in the absence of aggressive halide ions, the passive film maintains its passive state up to the electrode potential of oxygen evolution, i.e. ca. 1.0 V for stainless steel alloy [74,75], as illustrated by the dashed curve in Figure 2-3. Another important parameter that can be observed from a potentiodynamic polarization curve is the repassivation potential, E_R. As displayed in Figure 2-3, the concept of a repassivation potential against pitting is derived from the hysteresis loop generated by reversing the polarization scan direction at anodic potentials

above the pitting potentials and eventually crossing the forward curve in the passive region [73]. The electrode potential at this intersection is called the repassivation potential, which signifies the electrode potential at which the growth of active pits is diminished or possibly ceased, because the passive current density has been regained [73].

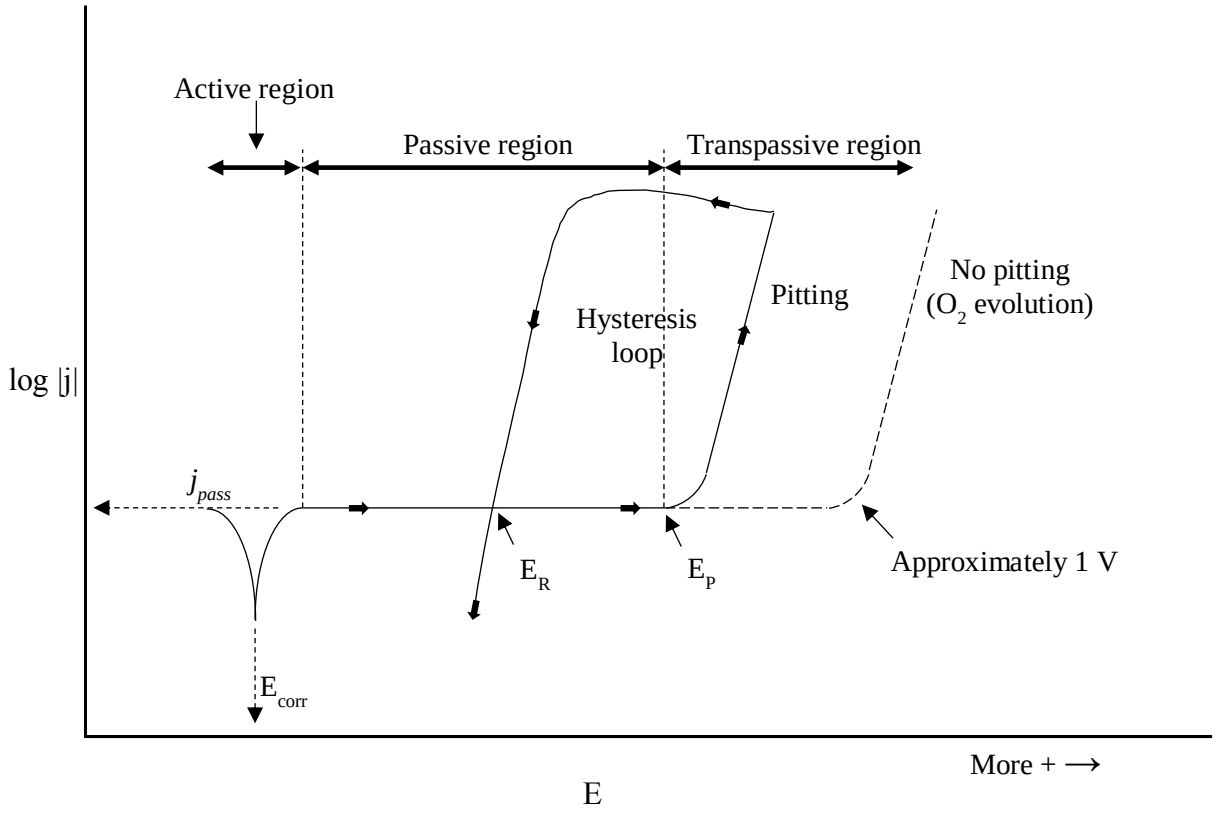

Figure 2-3 Schematic of a potentiodynamic polarization curve.

2.5 Current Methods for Controlling Corrosion of Biometallic Implants

Surface modification is one of the most viable options for improving the corrosion resistance of 316L SS implant devices. Surface modification has an advantage over other available methods, including using inhibitors or manufacturing new highly corrosion resistant alloys by modification of the bulk chemistry, because it can selectively achieve desirable surface properties while preserving the valuable properties of the bulk material [9]. As discussed earlier,

although 316L SS has an excellent bulk mechanical and physical properties, its poor localized pitting corrosion resistance has limited its applications as biomedical implants. Therefore, it is necessary to study the surface modification of 316L SS to obtain better surface chemistry and structure, and thus longer lifetime after implantation. A number of research groups have reported an enhancement of the corrosion resistance of stainless steels by applying various surface treatments. The most prevalent methods are ion implantation [10–12], bioactive ceramic coatings [13–16], electropolishing [17–19] and electrochemical passivation [20–24].

2.5.1 Bioactive Ceramic Coating

The application of bioactive coatings on metallic implants has been studied by many researchers using various coating techniques. In orthopedics and dentistry applications, bioactive ceramic coatings have received enormous consideration due to its advantages including enhanced corrosion resistance, bioactivity and osteointegration [76]. Hydroxyapatite (HAp) is the most common bioactive material for coating metallic implants used in orthopedics and dentistry due to the similarity of its crystal structural and composition with the inorganic matrix of the bone [77,78]. Several coating methods have been developed to deposit HAp onto a metallic surface, which include plasma spraying [77,79], hydrothermal deposition [78], sol-gel [80], electrophoretic technique [62] and electrochemical deposition [81]. In a corrosion study conducted by Fathi et al. [77], plasma sprayed HAp coating on 316L SS surface resulted in a positive shift in both open circuit potential and pitting potential when tested in a Ringer's solution. Moreover, it was also demonstrated that the two-layer coating composed of HAp/Ti on 316L SS was more corrosion resistant than the single HAp layer on 316L SS when tested in a 0.9 % NaCl solution [77]. However, plasma sprayed HAp coating has limitations in the clinical application on a load bearing implant because it can result in breaking or flaking off of the coating and may cause severe material degradation due to its poor mechanical properties [76]. By using other HAp deposition methods, researchers have reported to produce highly crystalline HAp coatings. For instance, Liu et al. [78] by employing a novel seeded hydrothermal deposition

method, showed that highly crystalline, dense, and adherent HAp coatings was obtained with this new method. Similarly, electrophoretic deposition technique was employed by Sridhar et al. [62] to achieve a uniform formation of the HAp coating on 316L SS. The electrophoretic deposition resulted in improved pitting resistance of 316L SS with 215 mV increase in the pitting potential for the HAp coated samples in comparison with untreated samples, evaluated in Hank's solution [62]. Apart from HAp coatings, different ions can also be substituted into the HAp lattice to improve the bioactive properties of the coating. This was done in a study by Sharifnabi et al. [14] in which fluoride and magnesium were successfully incorporated into apatite lattice structure by replacing hydroxide and calcium groups. The obtained Mg-substituted fluorapatite coatings resulted in a crack-free structure with crystallinity of about 70% and in a 149 nA/cm^2 decrease in corrosion current density, when tested in a Ringer's solution at 37 °C [14]. Similarly, Pourhashem and Afshar [15] produced double-layer coatings containing silica intermediate layer and a 45S5 bioglass (SiO_2-CaO-Na_2O-P_2O_5) top layer using the sol-gel method on 316L SS surface. The deposition of a bioglass-silica double-layer coating resulted in a 70 mV increase in corrosion potential and in a 1265 nA/cm^2 decrease in corrosion current density in comparison with uncoated surfaces.

2.5.2 Ion Implantation

Among various surface modification methods, ion implantation offers unique advantages such as the possibilities of introducing any kind of dopant into any solid material [10]. Anandan et al. [12] investigated the influence of nitrogen and oxygen ion implantation on the corrosion resistance of 205 stainless steel in 3.5% NaCl solution and their work showed that oxygen-implanted stainless steel resulted in an improvement in all corrosion parameters, while the corrosion resistance of nitrogen-implanted stainless steel became worse. Based on the Raman studies of oxide scales formed on the oxygen implanted stainless steel, they found that the improvement in the corrosion resistance was due to the formation of compact oxide composed of corundum and spinel form of oxides consisting of manganese, iron and chromium with

chromium enrichment at the surface of the resulting oxide structure [12]. In a similar study by Muthukumaran et al. [11], 316L SS was ion-implanted with nitrogen and helium and their analysis showed that both helium and nitrogen ion implantation resulted in an increase in pitting potential, when tested in 0.9% NaCl solution, from 92 mV on the control sample to 230 mV and 170 mV on the helium implanted and nitrogen implanted samples, respectively. Furthermore, the helium implanted sample showed a significant improvement in general corrosion behavior when compared to the bare sample, evidenced by an appreciable reduction in the corrosion current density, which is directly proportional to the corrosion rate, to 0.0689 mA/cm^2 from 1.2187 mA/cm^2 of the control sample [11].

2.5.3 Surface Passivation

The formation of a passive oxide film is dependent on the condition or atmosphere used for the film formation and also can be artificially varied with different surface passivation techniques. Acid dipping, also known as acid pickling, is one of the conventional surface passivation treatments used to remove impurities and contaminations on the surface using an aqueous solution of organic acid [82]. Noh et al. [83] reported that nitric acid passivation resulted in enhanced corrosion resistance of 316L SS, such that an increase in pitting potential by 150 mV was achieved when tested in 1 M NaCl at 70 °C. Their EDX and XPS analysis revealed that their result was due to both the enrichment of chromium oxide on the surface and partial removal of MnS inclusions from the surface [83]. Similarly, electrochemical and XPS studies of phosphoric acid treated 316L SS by Prabakaran and Rajeswari [84] showed that the acid treatment significantly increased corrosion resistance of 316L due to the enrichment of chromium oxide in the passive film. Moreover, it has been reported by Latifi et al. [18] that acid dipping can be used as a post-treatment step to yield higher chromium oxide enrichment in the oxide layer after the electropolishing treatment.

Among various surface passivation treatments, electrochemical polishing (EP) has been considered as an effective technique to enhance the corrosion resistance by producing a highly

homogeneous passive layer. EP involves an anodic dissolution process to reduce surface roughness and defects in an appropriate electrolyte [85]. The most common electrolytes currently employed in industry for the electropolishing of stainless steel are strong acid mixtures of phosphoric and sulphuric acid with varying concentrations [18,86]. Also, studies of electropolished 316L SS in other elaborated formulations with additives such as glycerol [17] and methanol [19] in phosphoric and sulphuric acid mixtures have reported improvement in surface roughness, topography and corrosion resistance. However, the resulting corrosion resistivity from electropolishing and acid pickling are still not adequate for biomedical applications, due to low pitting resistance.

A versatile alternative that can enhance the pitting corrosion resistance of metallic biomaterials is the use of electrochemical passivation by cyclic voltammetry, also known as cyclic potentiodynamic polarization [20–24]. CPP is based on the cyclic voltammetry method that enhances the passive properties of passive oxide films by sweeping the potential back and forth between two selected potentials, and the potential range is chosen such that it bounds the potential at which the electrochemical species is expected to oxidize or reduce. The distinct characteristic of cyclic voltammetry over other voltammetric techniques is in its ability to explore the electrochemical behavior of species generated at the electrode by scanning the potential in both anodic and cathodic directions. Hence, CPP can enhance the passive properties of surface oxide films by exploiting the kinetics of the redox reactions. Vukovic [20] reported enhanced stability of 302 stainless steel was achieved by repetitive potentiodynamic polarization in 1 M sodium hydroxide solution. Moreover, it has been reported by Shahryari et al. [22] that they have produced highly-protective passive oxide films on 316LVM stainless steel by employing the CPP technique. In their preliminary studies, they optimized the range of CPP parameters, including the number of polarization cycles and passivation electrolytes (deaerated solutions of 0.1 M phosphate buffer and 0.1 M $NaNO_3$ solutions), with respect to the passivation efficiency on both general and pitting corrosion [22]. In their results, the optimization of CPP conditions resulted in a significantly higher resistance to both general and pitting corrosion than that of the naturally formed passive film [22]. In fact, the results demonstrated that CPP-

modified passive film formed in the 0.1 M $NaNO_3$ electrolyte on the 316LVM surface was completely resistant to pitting corrosion in a physiological simulating solution [22].

2.6 Effects of Dissolved Oxygen on Passivation of 316L Stainless Steel

The formation of a passive oxide film on a stainless steel surface is a complex process that directly affects its corrosion behavior. Apart from alloying elements, the dissolved oxygen has been proposed as an effective factor that may have considerable effects on the mechanism of passive film formation and the passive film composition. Considerable research has been carried out to clarify the role of dissolved oxygen on the passivation of stainless steels. In general, the dissolved oxygen is known to have two different roles on the passivation phenomenon: (i) it acts as a cathodic depolarizer, which facilitates the kinetics of both anodic and cathodic passivation processes by reacting with the hydrogen gas surrounding the cathode and thereby speeding up the passivation process [25,26], and (ii) it act as a passivating agent by providing necessary chemical species for passivation [27,28]. Badea et al. [25] investigated the corrosion and passivation behavior of the 304 stainless steel in formic acid solutions at various concentrations in the absence and presence of dissolved oxygen and found out that the formic acid in the presence of dissolved oxygen promoted stability of the passivation for 304 stainless steel by inducing lower current density values, but they did not consider the oxygen as a passivating agent. This was in agreement with Raja et al. [26], who reported that the presence of dissolved oxygen in dilute sulfuric acid solution enhanced the passivation of 304 stainless steel but claimed that dissolved oxygen did not serve as a passivating agent since it apparently only provided the necessary potential for passivation but no chemical species necessary for passivation. In addition, Raja et al. [26] also reported that the passive films formed in presence and absence of dissolved oxygen exhibited similar charge carrier density and thus no effects of dissolved oxygen on charge carrier density were discovered. In contrast, Feng et al. [27] found that both anodic and cathodic processes were accelerated due to the effects of dissolved oxygen on charge carrier density. They discovered that the passive film of 316L SS formed in a borate buffer solution

saturated with dissolved oxygen contained more defects of oxygen vacancies than in the solution that had been deaerated [27]. This increase in density of oxygen vacancies allows more adsorption of anionic species such as NO_3^-, Cl^- and O_2^- and therefore an autocatalytic process of vacancy aided diffusion can occur [87]. As a result, more cationic and anionic movement through the passive film has facilitated the anodic and cathodic processes [27]. Similarly, Kim and Young [28] studied the effects of dissolved oxygen on the passive films grown on 316 stainless steel in NaCl solution and discovered that chemical species necessary for passivation are provided by dissolved oxygen since the density of oxygen vacancies was higher for the passive film formed in non-deaerated solution compared to that formed in deaerated solution. However, despite considerable research mentioned above, the effects of dissolved oxygen on the passivation mechanism are inconsistent and depend on the electrochemical systems involved in the types of materials and solutions. Hence, the role of dissolved oxygen on the passivation of stainless steels still remains unclear.

CHAPTER 3: OBJECTIVES

The main objective of the present research was to optimize an electrochemical surface modification method called cyclic potentiodynamic polarization for the formation of highly corrosion resistant passive oxide film on a 316L stainless steel surface using 0.1 M $NaNO_3$ solution as a passivation electrolyte, in deaerated and aerated conditions. Also, the effect of dissolved oxygen on the passivation efficiency of the CPP technique was investigated by evaluating corrosion resistance of the modified surfaces formed in the absence and presence of dissolved oxygen. The influence of number of cyclic passivation sweeps on the passivation efficiency was investigated with the aim of achieving high resistance to both general and pitting corrosion in a phosphate buffered saline solution pH 7.4 containing 0.027 M KCl and 0.137 M NaCl (simulating body-fluid). The resulting corrosion behavior of the modified surface was analyzed using electrochemical techniques such as open circuit potential (OCP) measurements and potentiodynamic polarization tests.

The main objectives were achieved by accomplishing the following specific objectives:

I. Optimization of CPP technique for the formation of highly corrosion resistant passive oxide film on a 316L SS surface using 0.1 M $NaNO_3$ solution in deaerated and aerated conditions by investigating the influence of number of cyclic sweeps on the resulting general and pitting corrosion behavior.
II. Investigation of the effect of dissolved oxygen on the passivation efficiency and the corrosion resistance of 316L SS using OCP measurements and potentiodynamic polarization tests.

CHAPTER 4: MATERIALS AND EXPERIMENTAL METHODS

4.1 Electrode Preparation

The specimens were prepared from a solid rod of 316L stainless steel (McMaster-Carr) with diameter of a 12.7 mm. The rod was cut into 3 mm thick discs and embedded in epoxy resin after soldering copper wire on their backsides. The chemical composition of 316L SS is presented in Table 4-1. Prior to electrochemical tests, the 316L SS samples were wet-polished using 600 grit abrasive paper, then rinsed with deionized water, sonicated in ethanol for 5 minutes to remove surface polishing residues, and finally dried with argon gas.

Table 4-1 Chemical composition of AISI 316L stainless steel (in wt.%).

Element	Composition (in wt. %)
Fe	Bal.
C	0.03
Mn	2.00
P	0.045
S	0.03
Si	1.00
Cr	18.00
Ni	14.00
Mo	3.00

4.2 Electrochemical Setup

All electrochemical tests were carried out using a conventional three-electrode electrochemical cell, as illustrated in Figure 4-1. In this setup, the 316L SS samples, a saturated calomel electrode (SCE, 0.242 V vs. standard hydrogen electrode), and a graphite rod were used as working, reference, and counter electrodes, respectively. All potentials were measured with respect to SCE. All electrochemical measurements were performed on a computer-controlled Autolab PGSTAT30/FRA2 Potentiostat/Galvanostat electrochemical system using NOVA 2.1 software (Metrohm Autolab).

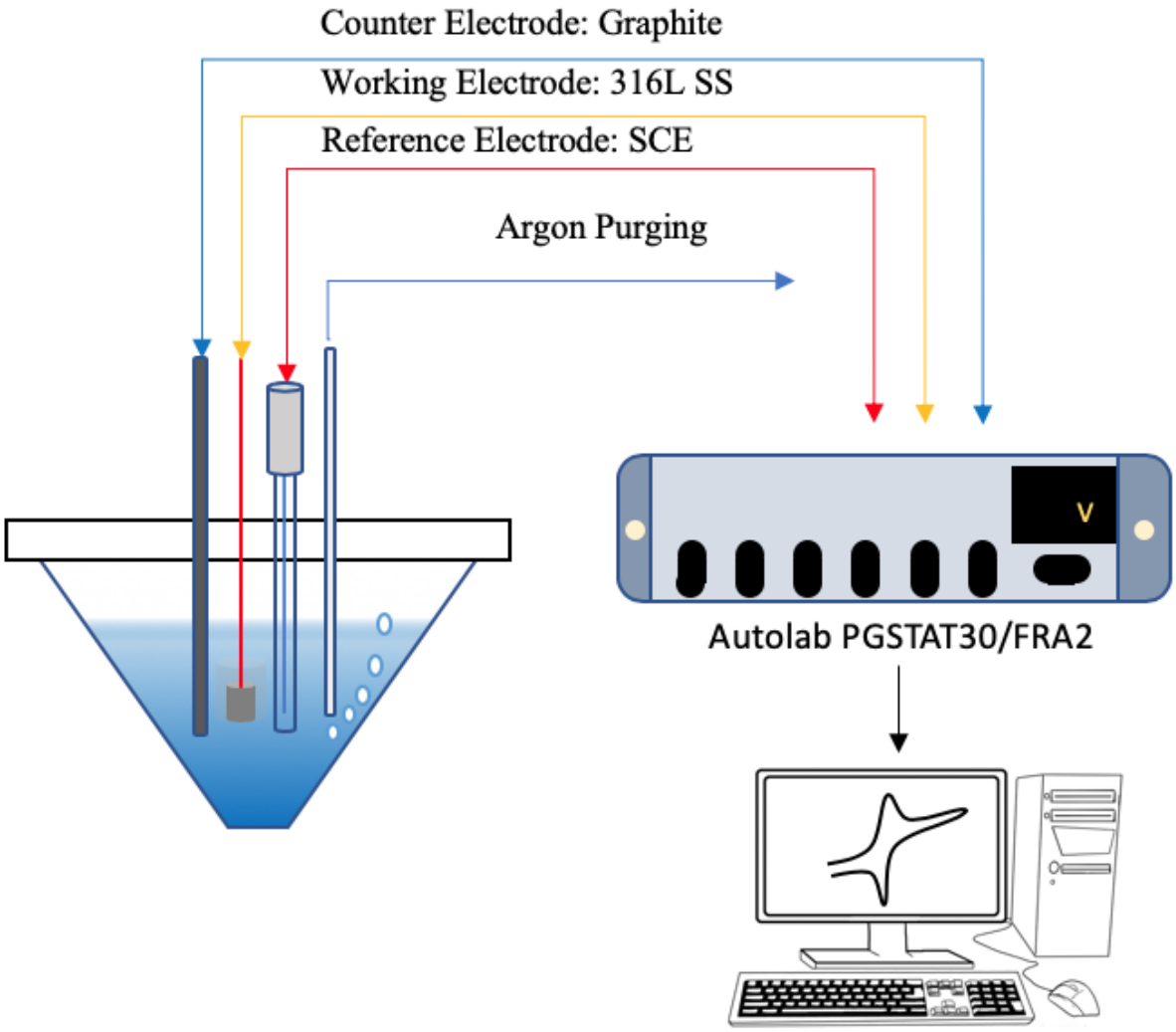

Figure 4-1 Three electrodes electrochemical cell assembly.

For passivation of 316L SS samples, 0.1 M $NaNO_3$ solution in deaerated condition and in aerated condition were used as passivation electrolytes. The corrosion behaviour of the 316L SS samples were evaluated in phosphate buffered saline (PBS) solution (pH 7.4, containing 0.027 M KCl and 0.137 M NaCl) and the tests were conducted in deaerated environment. The chemical composition of the PBS solution was selected from ASTM standards (F2129) and is shown in Table 4-2. For all deaerated tests, the electrolyte was purged with argon gas (99.998% pure) for 1 h prior to testing and then continuously throughout the test. Deionized water (resistivity of 18.2

MΩcm) was used in the preparation of all aqueous solutions. All experiments were carried out at room temperature (22 ± 1°C).

Table 4-2 Chemical composition of the PBS solution.

Chemical	Composition (g L^{-1})
NaCl	8.0
KCl	0.2
Na_2HPO_4	1.15
KH_2PO_4	0.2

4.3 Electrochemical Techniques

Electrochemical passivation of a 316L SS surface was performed using the CPP technique in 0.1 M $NaNO_3$ solution in the absence and presence of dissolved oxygen. The main parameters of the CPP procedure employed in the present research are essentially the same as the work previously done in our lab with minor adjustments [22]. Prior to each passivation experiment, the working electrode (WE) was cathodically polarized at -0.8 V for 5 s in order to reduce the surface oxides formed naturally during the electrode preparation steps. Then, CPP was applied in the potential range between -0.8 V and 0.9 V at a scan rate of 100 mV s^{-1}. Depending on the type of passivation electrolyte used, the samples passivated in 0.1 M $NaNO_3$ solution under deaerated condition or aerated condition were named as "EM-DC" or "EM-AC", respectively. The samples without the application of CPP passivation were denoted as “unmodified” WE surface. Prior to electrochemical experiments, the interstices on the WE surface between the 316L SS specimen and the epoxy resin were coated with nail-polish (acrylic) in order to avoid crevice corrosion.

The corrosion analysis of the naturally grown (“unmodified”) and electrochemically-passivated ("EM-DC" and "EM-AC") 316L SS surfaces were performed using open circuit potential (OCP) measurements and potentiodynamic polarization tests. An OCP measurement was carried out first, for 1 h. Then, a potentiodynamic polarization measurement was conducted

at a scan rate of 1 mV/s and the potential was applied from -100 mV vs. OCP to a potential at which the current density was 1 mA/cm^2. After reaching this point, the polarization sweep was reversed back to the initial potential. After each corrosion experiments, the surface area of the working electrode exposed to the electrolyte was determined. All experiments were repeated for at least 3 times to ensure reproducibility and the reported error bars are based on standard deviations.

CHAPTER 5: RESULTS AND DISCUSSIONS

5.1 Cyclic Potentiodynamic Polarization

As stated in the introduction, the main goal of the present research was to enhance the passive properties of the 316L SS surface by using the CPP method. Figures 5-1 and 5-2 display the cyclic voltammograms of 316L SS electrodes recorded in deaerated and aerated 0.1 M $NaNO_3$ solutions, respectively. The cyclic voltammograms were recorded in a potential region between -0.8 to 0.9 V, in which the solid curve represents the 1st polarization sweep and the dashed curve represents the 200th polarization sweep. As can be seen in Figures 5-1 and 5-2, the shapes of the cyclic voltammograms measured in both deaerated and aerated conditions undergo considerable changes with the increase in the number of polarization sweeps. The peaks/shoulders appearing in a cyclic voltammogram corresponds to a particular redox reaction, and the height of a peak current is proportional to the extent or magnitude of that reaction. The 1st polarization sweep of cyclic voltammogram for 316L specimen recorded in the deaerated $NaNO_3$ solution (Figure 5-1) shows two small anodic humps at -600 mV (A_1) and -200 mV (A_2), one anodic peak at 600 mV (A_3), one small cathodic shoulder at -450 mV (C_1) and one cathodic peak at -50 mV (C_2), respectively. Similar shape was observed for the 1st polarization sweep of the voltammogram recorded in the aerated condition (Figure 5-2), which shows one small anodic shoulder at -450 mV (A_1), two anodic shoulders at 0 mV (A_2) and 600 mV (A_3), one small cathodic shoulder at -450 mV (C_1) and one cathodic peak at -50 mV (C_2). The shapes of the cyclic voltammograms (Figures 5-1 and 5-2), or more specifically the correlation between the peaks to specific redox reactions, obtained in the present research are in good agreement with previous findings reported in literature [74,75,88,89]. In the anodic polarization direction, the anodic shoulder A_1 could be attributed to the electroformation of a $Fe(OH)_2$ layer on the pre-existing Cr(III) containing oxide layer [74,75]. Around -200 mV and 0 mV, another anodic current feature A_2 can be observed, which could be the oxidation of Fe(II) into Fe(III)-species (i.e. Fe_2O_3) [74,75]. After A_2, the voltammogram ascends gradually to a broad anodic shoulder A_3. This could be attributed to the oxidation of Cr(III)-oxide into soluble Cr(VI)-species (i.e. $Cr_2O_7^{2-}$) in the potential range of the current peak A_3 [74,75]. In the reverse cathodic polarization scan, the peak C_2 could be attributed to the reduction of Cr(VI)-species back to Cr(III)-oxide in

the passive film and the shoulder C_1 could be related to the reduction of Fe(III) to Fe(II)-species [74,75]. The high current densities at -800 mV and 900 mV are due to hydrogen evolution and oxygen evolution, respectively [74,75].

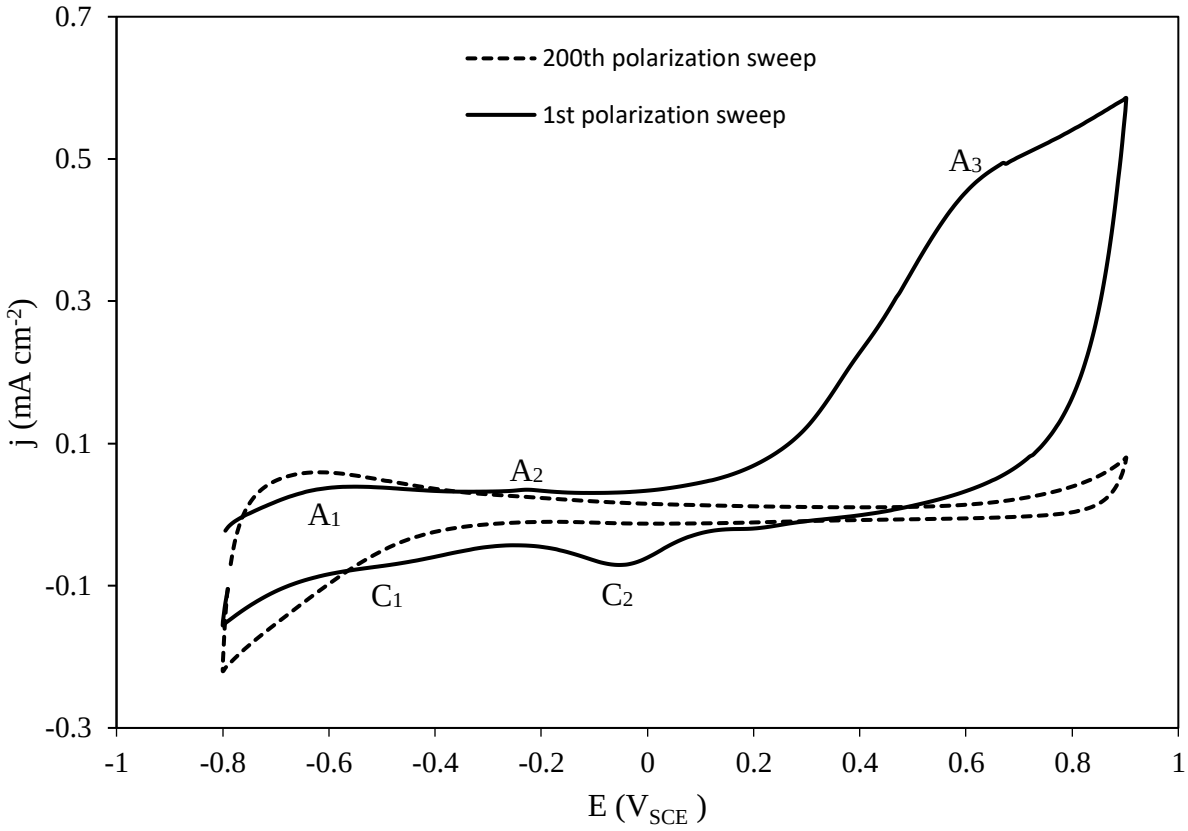

Figure 5-1 Cyclic voltammograms of the 316L stainless steel electrodes recorded in deaerated 0.1 M $NaNO_3$ solution. The solid curve represents the 1st polarization sweep and the dashed curve represents the 200th polarization sweep. Scan rate = 100 mVs^{-1}.

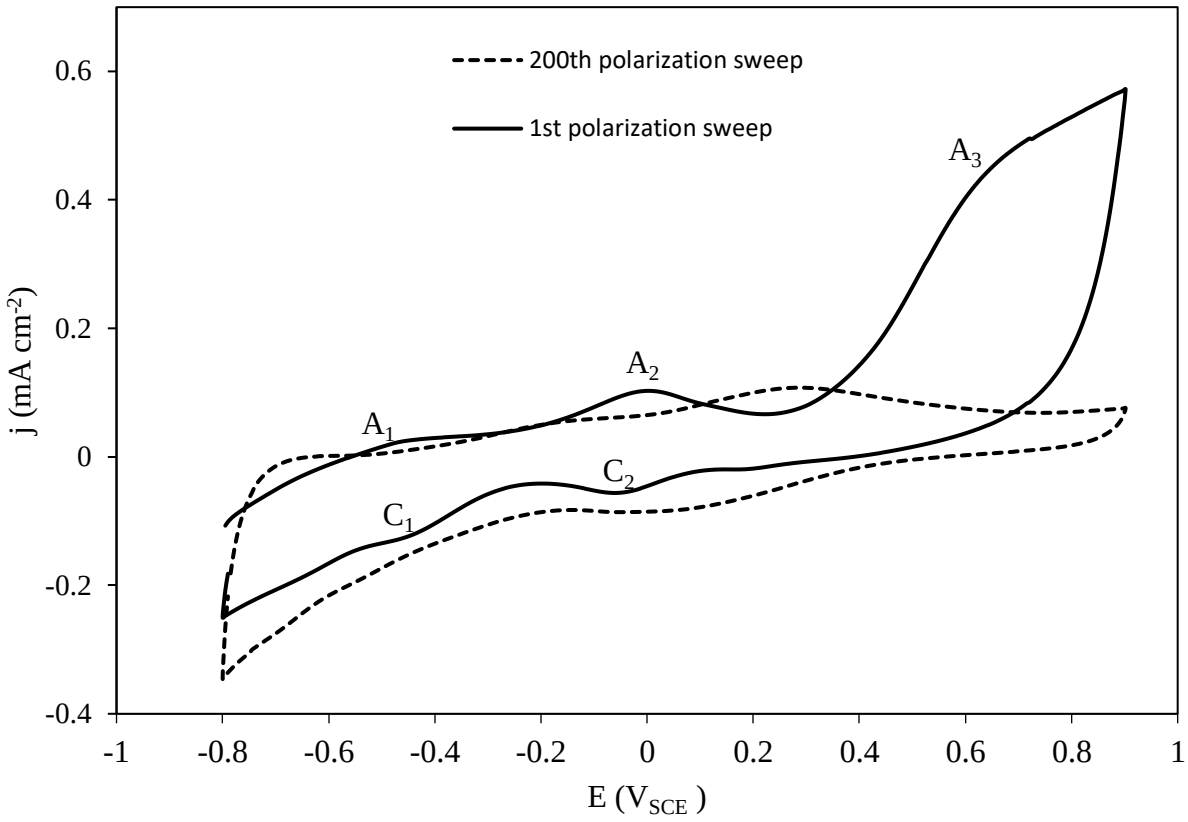

Figure 5-2 Cyclic voltammograms of the 316L stainless steel electrodes recorded in aerated 0.1 M $NaNO_3$ solution. The solid curve represents the 1st polarization sweep and the dashed curve represents the 200th polarization sweep. Scan rate = 100 mVs^{-1}.

The interpretation of the cyclic voltammograms is mainly derived from the relation of the shape and the size of the peaks to the specific redox reactions. The 1st polarization sweeps of both voltammograms (Figures 5-1 and 5-2) clearly show that polarization in both conditions (i.e. deaerated and aerated) have irreversible behavior. As seen in Figure 5-1, in deaerated condition, the 1st sweep shows that the oxidation peak of Cr(III)-oxide to Cr(VI)-species (A_3) is relatively bigger and broader than the reduction peak of Cr(VI)-species to Cr(III)-oxide (C_2). Likewise, the 1st sweep recorded in aerated condition displays similar behavior in the peak height and size. These results imply that the Cr(VI)-species formed during the first anodic polarization sweep are mostly dissolved in the solution. Furthermore, the larger anodic current features of the 1st polarization sweeps of both voltammograms (Figures 5-1 and 5-2) suggest that the pre-formed

passive film on the freshly polished 316L surface is very thin and highly susceptible to dissolution in the aqueous phase. However, with increasing the number of polarization sweeps, smaller (narrower) voltammograms (Figures 5-1 and 5-2) can be observed for both deaerated and aerated conditions. In fact, this behavior is more predominant for the cyclic polarization under deaerated condition (Figure 5-1). In either case, the voltammograms (Figures 5-1 and 5-2) display the reduction of current densities, which is the indicator of higher resistance of passive film, after the 200th polarization sweep. This outcome suggests that thicker and probably more structured passive films are formed on increasing the number of sweeps, hence less susceptible to dissolution. In addition, as a result of the cyclization of the 316L electrode, the reversibility of the redox reactions has improved significantly after the 200th polarization sweep, which is illustrated by the redox current peaks having relatively equal size.

In order to gain more quantitative understanding on the effects of the cyclic polarization on the 316L electrode, the ratio of the total anodic-to-cathodic charge is presented in Figures 5-3 and 5-4. As it was previous mentioned, the relatively larger anodic current features of 1st polarization sweeps of both voltammograms (Figures 5-1 and 5-2) suggest that the redox reactions are irreversible. This is certainly the case as the ratio of the total anodic-to-cathodic charge in the first cycles is Q_A/Q_C =17.97 for deaerated condition and Q_A/Q_C =5.3 for aerated condition. Moreover, the ratios indicate that only ca. 6% and ca. 19% of the charge related to the anodic reactions are used to form metal oxide species that constitute the passive film and are the reduced during the cathodic polarization for deaerated and aerated conditions, respectively. However, as displayed by Figures 5-3 and 5-4, the reversibility of the redox reactions significantly improves with the cyclic polarization of the surface. Under deaerated and aerated conditions (Figures 5-3 and 5-4, respectively), the reversibility of the anodic processes reaches 100% after 30th sweep and 1st sweep, respectively. This result indicates possible improvement in the passive properties of the passive film formed under both deaerated and aerated conditions since the 100% reversibility indicates that the anodic dissolution of the passive film into the solution is completely eliminated. Furthermore, it is observed that the cyclic polarization of the 316L surface under aerated condition is more efficient in enhancing the passive properties since the reversibility of the redox reactions is reached immediately after the 1st polarization sweep.

Hence, this demonstrates compelling evidence for the positive effect of dissolved oxygen on the passivation of 316L SS surface by CPP method. In accordance with the report by Feng et al. [27], the dissolved oxygen seems to have facilitated the anodic and cathodic processes by promoting more cationic and anionic movement through the passive film. Next, OCP and pitting polarization measurements were performed to investigate the effect of CPP on the resulting corrosion behaviour of the 316L SS surface.

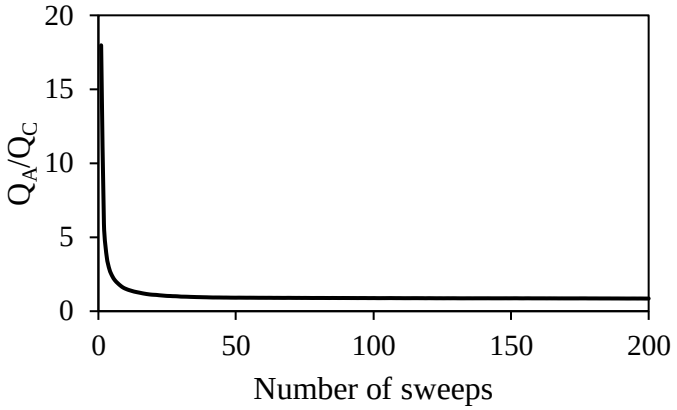

Figure 5-3 Variation of the anodic-to-cathodic total charge ratio with the number of sweeps for the 316L stainless steel electrodes modified by CPP method in deaerated 0.1 M $NaNO_3$.

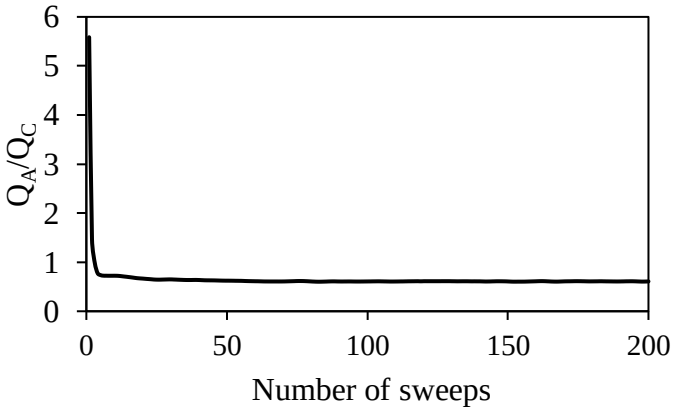

Figure 5-4 Variation of the anodic-to-cathodic total charge ratio with the number of sweeps for the 316L stainless steel electrodes modified by CPP method in aerated 0.1 M $NaNO_3$.

5.2 Open Circuit Potential

The open-circuit-potential (OCP) measurement was conducted to examine the influence of CPP on the surface potential of the electrode. A more positive OCP indicates higher resistance of the material to general corrosion. Figure 5-5 depicts the changes in OCP as a function of immersion time in PBS solution at 22 °C for the unmodified and EM-DC 316L SS samples. As can be seen in Figure 5-5, an abrupt drop in the potential of the unmodified surface was observed during the first seconds of immersion and then the potential starts to fluctuate for 1000 s and gradually shifts towards more noble values. Such an OCP profile indicates that the passive film of the unmodified sample was gradually stabilizing after undergoing dissolution for duration of 1000 s. Similar OCP stabilization behavior of unmodified 316L SS were reported by Omanovic and Roscoe [90] and Karimi et al. [91]. In contrast, the EM-DC surface passivated for 25 cycles displayed an abrupt increase in the OCP during the first seconds of immersion and then a steady behavior during the rest of the measurement. In fact, as the number of cyclic sweeps applied on the EM-DC surfaces increased, there was an increase in the extent and the duration of the rapid rise in the OCP during the beginning of the measurement (Figure 5-5). Most importantly, with the increase in the number of CPP cycles, the OCP measured on the EM-DC surfaces shifted to more noble potentials (Figure 5-6). This result indicates that CPP has effectively enhanced the corrosion stability of the protective passive film on the surface of the alloy by possibly inducing higher chromium-oxide content in the film, which is the main factor responsible for the high corrosion resistance of 316L SS [1,22,35,40,45].

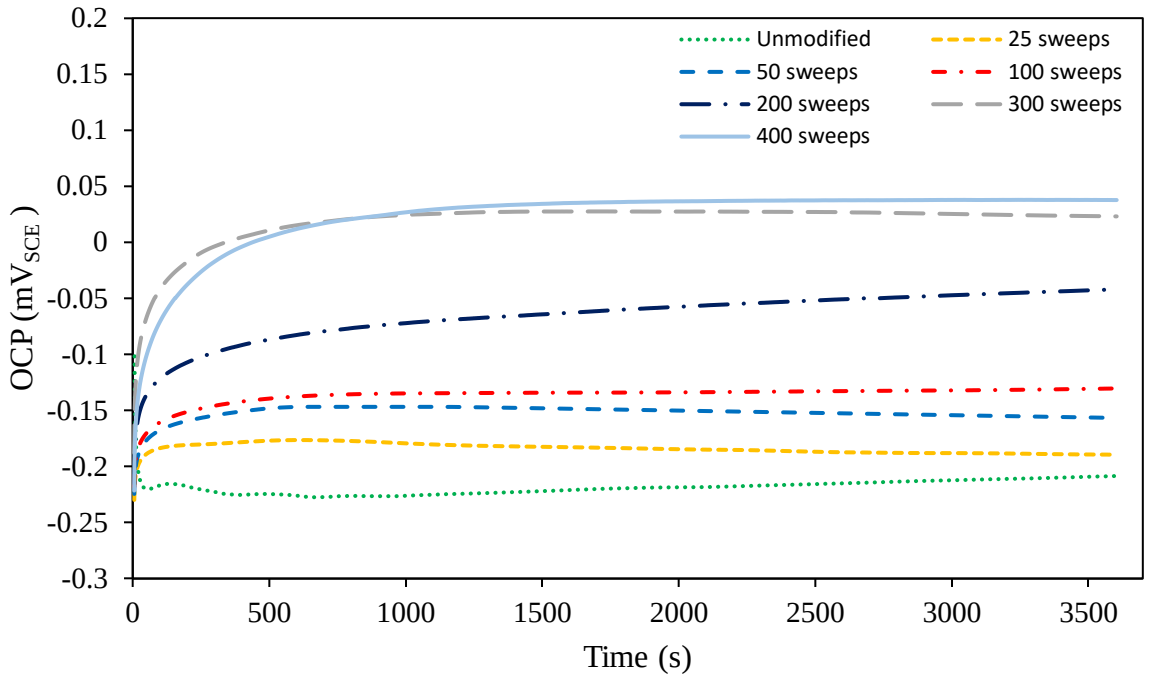

Figure 5-5 Open circuit potential measurements of the unmodified and EM-DC 316L surfaces recorded in a PBS solution pH 7.4 containing 0.027 M KCl and 0.137 M NaCl. The modification of the surfaces was done by cyclic potentiodynamic polarization in deaerated 0.1 M $NaNO_3$ solution between -0.8 V and 0.9 V at a scan rate of 100 mVs^{-1} by applying the specified number of sweeps.

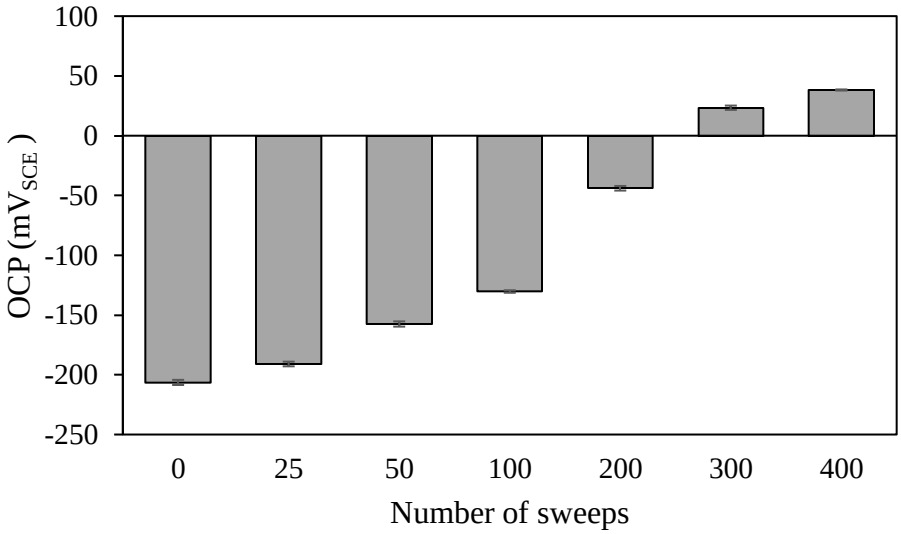

Figure 5-6 Dependence of OCP on the number of sweeps applied during the modification of the 316L surface in deaerated condition. The values are obtained from Figure 5-5 after one hour.

Similar to the results obtained for EM-DC surfaces, with the increase of the number of cycles, the OCP values obtained for the EM-AC surfaces shifted to more noble potentials, which again reflects the positive influence of CPP on enhancing the steady-state corrosion potential of the surfaces (Figures 5-7 and 5-8). Furthermore, the notable observation from the OCP data comparison between the EM-DC and EM-AC surfaces (Figures 5-6 and 5-8) is that the OCP values obtained for the EM-AC surfaces are significantly higher than those of the EM-DC surfaces for each respective number of cycles. In comparison, the OCP value of the EM-AC sample passivated for 25 cycles is ca. 61.5 mV nobler than that of the EM-DC sample passivated for 400 cycles. This shows, as it was suggested in the previous section, that the CPP method employed in the aerated condition is significantly more efficient in passivating the 316L SS surfaces than in the deaerated condition. Furthermore, these results indicate that the factor that may be responsible for significantly increasing the passivation efficiency of CPP method is the presence of dissolved oxygen in the passivation electrolyte. As discussed previously, the dissolved oxygen seems to have a positive effect on the passive film formation by enhancing the passivation efficiency of CPP method by facilitating more cationic and anionic movement through the passive film [27]. In fact, Khobragade et al. [87] reported that dissolved oxygen has the tendency to increase the density of oxygen vacancies on the passive film, which can allow more adsorption of anionic species such as NO_3^-. As a result, this could have catalyzed the passivation process by possibly inducing more vacancy aided diffusion.

In brief, OCP measurements indicate that CPP could be a highly effective surface modification method for improving the general corrosion resistance of 316L SS. Moreover, these results also reveal that the effectiveness of the CPP method on the passivation of 316L surface increases with the incorporation of dissolved oxygen in the passivation electrolyte.

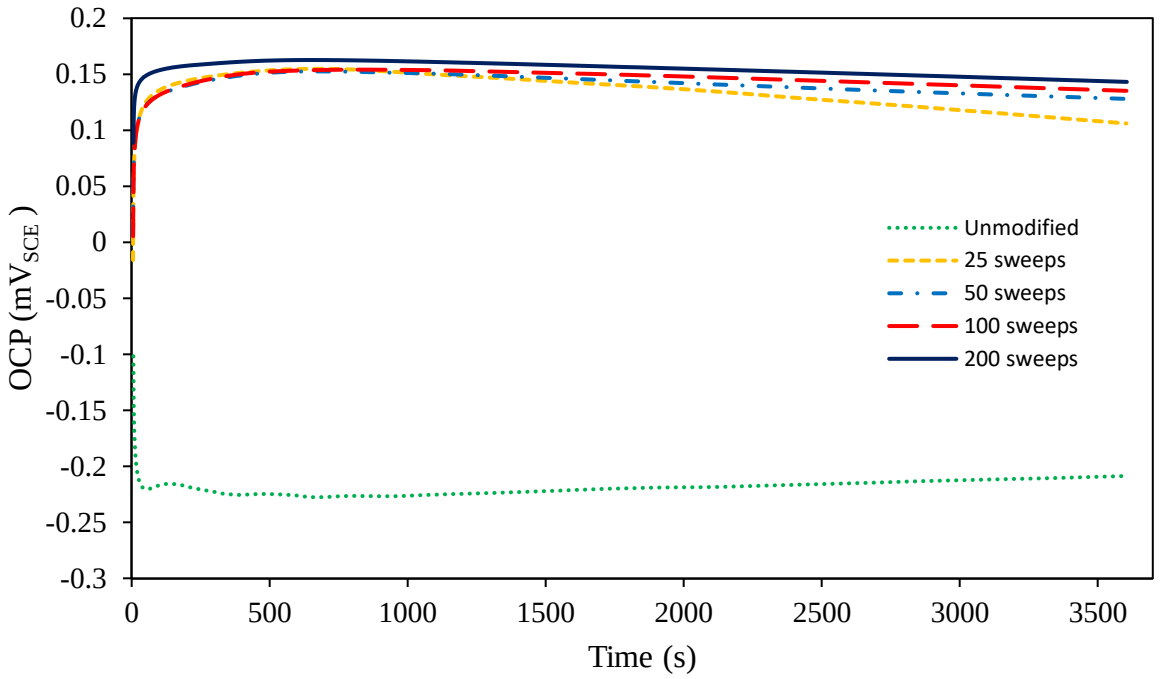

Figure 5-7 Open circuit potential measurements of the unmodified and EM-AC 316L surfaces recorded in a PBS solution pH 7.4 containing 0.027 M KCl and 0.137 M NaCl. The modification of the surfaces was done by cyclic potentiodynamic polarization of the electrodes in aerated 0.1 M $NaNO_3$ solution between -0.8 V and 0.9 V at a scan rate of 100 mVs^{-1} by applying the specified number of sweeps.

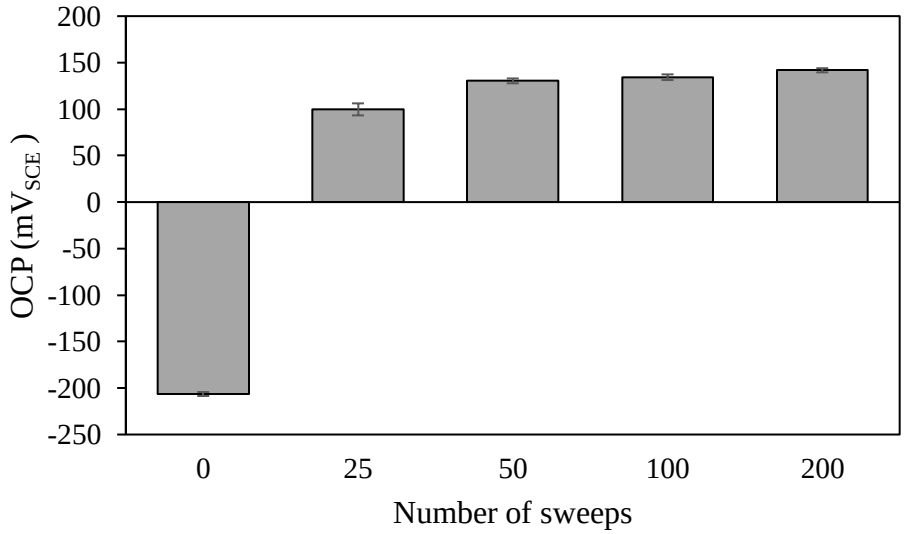

Figure 5-8 Dependence of OCP on the number of sweeps applied during the modification of the 316L surface in aerated condition. The values are obtained from Figure 5-7 after one hour.

5.3 Pitting Corrosion Resistance

In the present research, potentiodynamic polarization tests were performed to evaluate the pitting corrosion susceptibility of the unmodified, EM-DC and EM-AC 316L SS surfaces by measuring the pitting potential.

The potentiodynamic polarization curves recorded for EM-DC samples in deaerated PBS solution are presented in Figure 5-9. The figure shows that CPP improves the corrosion properties of the 316L SS surface by decreasing the passive current density (the 'semi-horizontal' region of the curve) and by significantly increasing the pitting potential (the point of abrupt increase in current). Thus, passive current densities of the EM-DC sample passivated for 400 cycles are almost two orders of magnitude lower than those for the unmodified sample, indicating a significant improvement in the protective properties of the passive oxide film. More importantly, a considerable improvement in pitting resistance is observed for EM-DC surfaces with increase in the number of cyclic sweeps applied on its surface. The CPP method improves the pitting potential of the unmodified surface from ca. 0.376 V to ca. 1.0 V with passivation of 200 cyclic sweeps. In fact, the rise in current at 1.0 V was due to oxygen evolution, rather than the initiation of pitting corrosion [22,74,75]. However, as can be seen in Figure 5-9, the polarization curve recorded on EM-DC surface passivated for 200 sweeps displays pitting during the return polarization scan after its reversal point. This indicates that the passivation by CPP technique have led to improvement of the passive oxide film, which results in the absence of pitting in the forward-going scan. However, at high potentials, there is a formation of meta-stable pits that becomes more progressive as the sample is kept within the transpassive region, which results in the breakdown of the film and its pitting in the returning scan. Hence, further investigation of the EM-DC surface with higher number of cyclic sweeps than 200 was conducted. The polarization curves recorded on EM-DC surfaces passivated for 300 and 400 sweeps are also presented in Figure 5-9. The results show that there were no distinct changes in the pitting behavior obtained for the EM-DC surfaces passivated for 200, 300 and 400 sweeps and no further improvement in terms of pitting resistance was observed with increasing the

number of cyclic sweeps above 200. Hence, this demonstrates that there is a limitation on the enhancement of pitting resistance of 316L SS by CPP technique using a deaerated 0.1 M $NaNO_3$ solution.

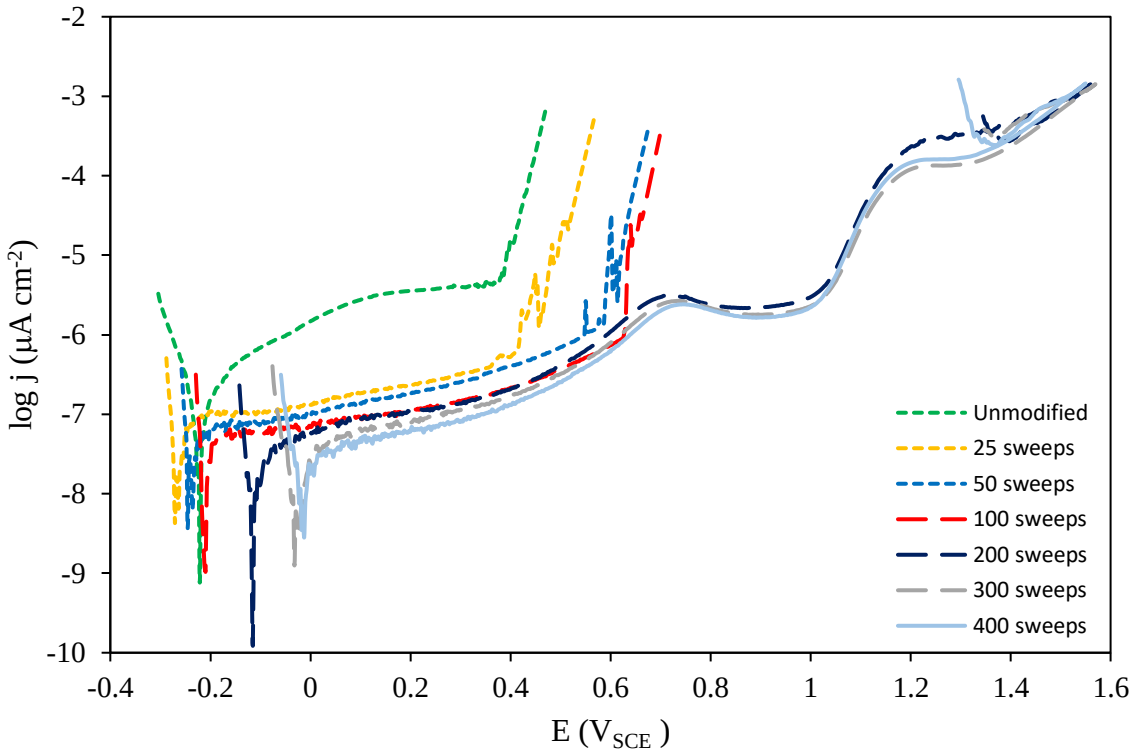

Figure 5-9 Potentiodynamic polarization curves of the unmodified and EM-DC 316L surfaces recorded in a PBS solution pH 7.4 containing 0.027 M KCl and 0.137 M NaCl. The modification of the surfaces was done by cyclic potentiodynamic polarization of the electrodes in deaerated 0.1 M $NaNO_3$ solution between -0.8 V and 0.9 V at a scan rate of 100 mVs^{-1} by applying the specified number of sweeps.

Figure 5-10 more clearly presents the dependence of pitting potential on the number of passivation cycles. It is observed that the pitting potential of the EM-DC surfaces improves with the increase in the number of cyclic sweeps applied, and that there is, thus, a significant influence of the number of sweeps on the resulting pitting behaviour. This shows that CPP is indeed an effective surface modification method for improving the pitting resistance of 316L SS.

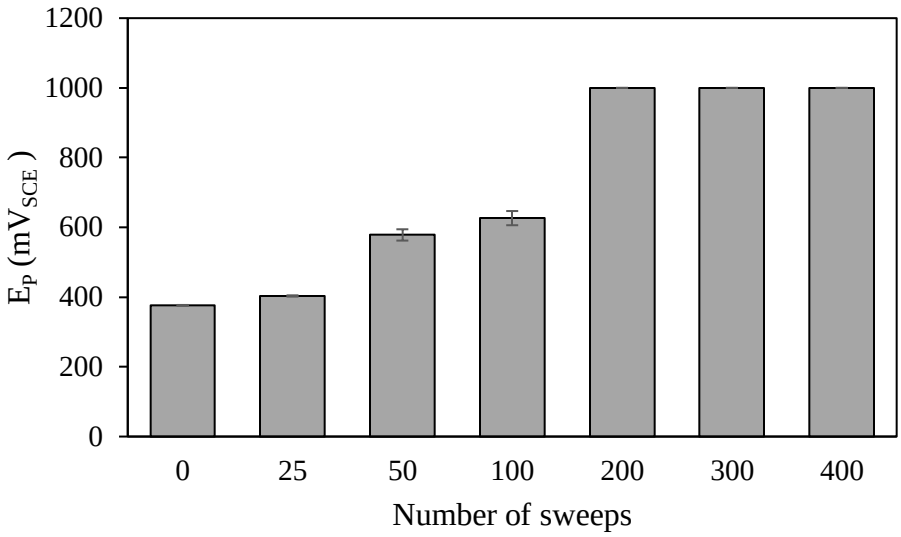

Figure 5-10 Dependence of the pitting potential on the number of sweeps applied during the modification of the 316L surface. The values are obtained from curves presented in Figure 5-9.

The potentiodynamic polarization curves of EM-AC samples passivated at different number of cyclic sweeps are shown in Figure 5-11. In accordance with the EM-DC samples, the passive current densities (semi-horizontal parts of the curves) of the EM-AC samples demonstrate a reduction from that of the unmodified sample. However, the passive current densities of the EM-AC samples are one order of magnitude greater than that of the EM-DC samples, indicating that these samples are less resistant to general corrosion. On the other hand, it is observed that the pitting potential of EM-AC samples increases with higher number of cyclic sweeps applied on its surface. Although the EM-AC samples resulted in greater passive current densities than the EM-DC samples, higher pitting potential was achieved with the EM-AC samples, indicating better pitting corrosion resistance. As can be seen in Figures 5-10 and 5-12, at each specified number of polarization sweeps, the EM-AC samples exhibit higher pitting potentials than the EM-DC samples. These results are in agreement with the results obtained from OCP measurement. Furthermore, as shown in Figure 5-11, the EM-AC surface passivated for 200 sweeps displays a complete absence of pitting during its returning scan. The increase in potential at around 1V is due to the onset of oxygen evolution reaction and trans-passive behaviour of the material. Further investigation in the higher number of cyclic sweeps, i.e. 300

sweeps for EM-AC sample, resulted in the same corrosion behavior as the EM-AC sample with 200 sweeps. This result shows that the passive oxide film formed by CPP technique using an aerated 0.1 M $NaNO_3$ solution is completely resistant to pitting corrosion in a deaerated PBS solution at 22 °C. Hence, this result along with the OCP measurements indicate that dissolved oxygen has a positive effect in the passivation of 316L SS by CPP method.

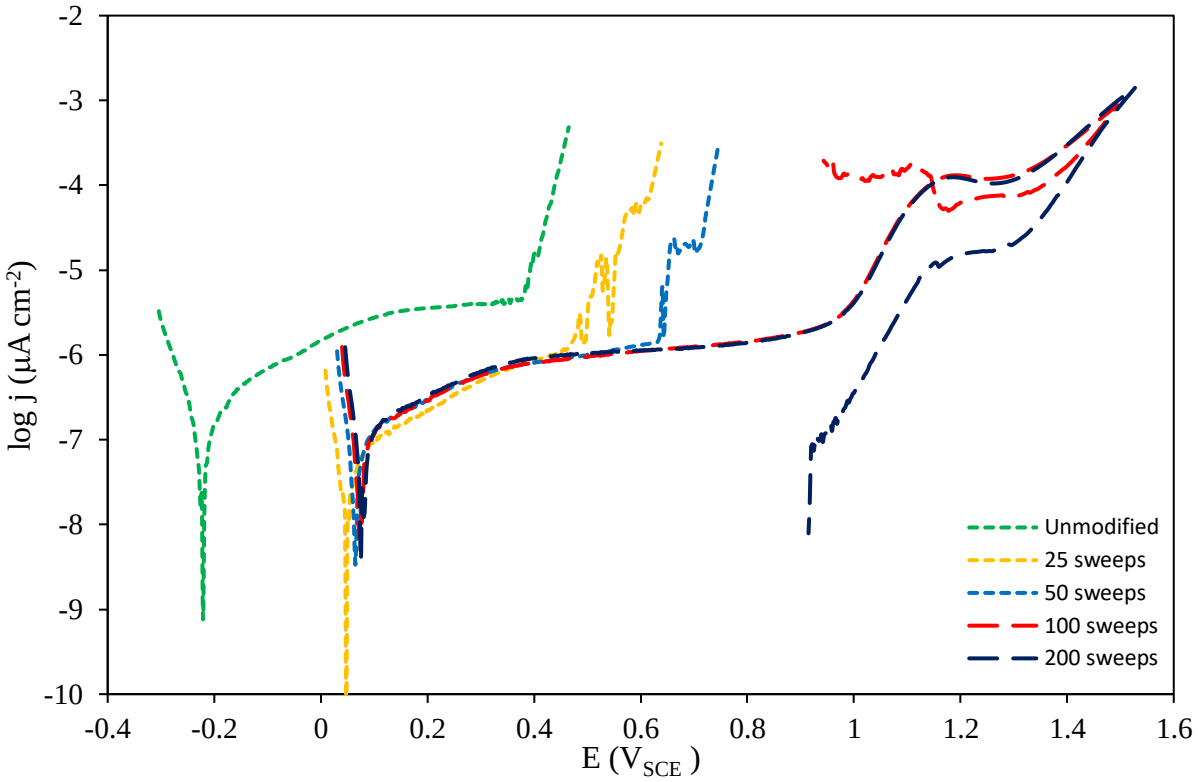

Figure 5-11 Potentiodynamic polarization curves of the unmodified and EM-AC 316L surfaces recorded in a PBS solution pH 7.4 containing 0.027 M KCl and 0.137 M NaCl. The modification of the surfaces was done by cyclic potentiodynamic polarization of the electrodes in aerated 0.1 M $NaNO_3$ solution between -0.8 V and 0.9 V at a scan rate of 100 mVs^{-1} by applying the specified number of sweeps.

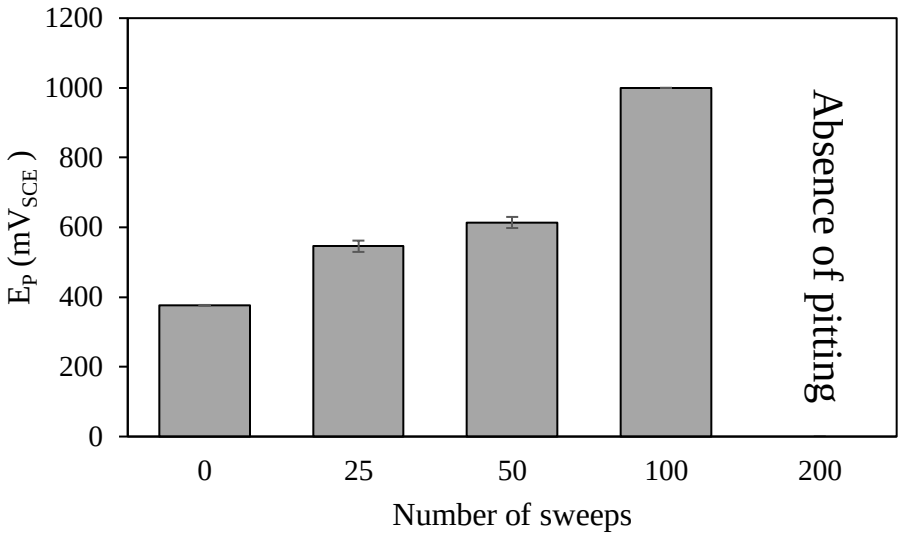

Figure 5-12 Dependence of the pitting potential on the number of sweeps applied during the modification of the 316L surface. The values are obtained from curves presented in Figure 5-11.

The results presented in the present research correlate well with the previous findings in the literature by Shahryari et al. [22] and further support the application of CPP for surface modification of austenitic stainless steels. Further measurements are needed in order to explain the origin of improvement in pitting corrosion resistance of 316L presented above. Namely, improved corrosion resistance of the 316L surface modified by CPP could be due to several factors such as changes in the surface chemical composition, semiconducting properties, structure, and roughness [1,22,35]. As discussed earlier, the chromium-oxide enrichment in the outer layer of the passive film on the 316L surface modified by CPP is mainly responsible for corrosion resistance of the alloy due to the change in the semiconducting/electronic structure of passive film [1,22,35,40,45]. This is because the *p*-type semiconducting properties of the chromium oxides, which are characterized by an excess of cation vacancies, repels the corrosion attacks from aggressive halide anions [7,8]. Therefore, as reported in previous studies [21,22], the increase of the Cr/Fe ratio in the outer passive layer of 316L SS after the CPP process could be associated with the results obtained in the present research.

CHAPTER 6: CONCLUSIONS

The present research investigated the efficacy of cyclic potentiodynamic polarization technique using 0.1 M $NaNO_3$ solution as a passivation electrolyte in deaerated and aerated conditions, as a surface modification method for the improvement of pitting corrosion resistance of 316L stainless steel. The resulting corrosion behavior of the materials was evaluated in a physiological simulating electrolyte (0.1 M PBS) at 22 °C. Also, the influence of dissolved oxygen on the passivation efficiency of the CPP method was evaluated.

It was found that the CPP method under both deaerated and aerated conditions enabled the formation of a passive oxide film that offers a significantly higher pitting corrosion resistance than the naturally grown passive film. The key findings of this work are summarized in the following:

I. CPP improves the corrosion resistance of the 316L SS surface, as demonstrated by an increase in OCP, a decrease in the passive current density and a significant increase in pitting potential.
II. It was observed that dissolved oxygen has a positive effect on the passivation of 316L SS under CPP conditions.
III. The 316L SS surface passivated for 200 sweeps in aerated 0.1 M $NaNO_3$ solution exhibited largest improvement: highest open circuit potential (141.77 mV_{SCE}) and complete resistance to pitting corrosion in a 0.1 M PBS solution at 22 °C.

REFERENCES

[1] J.R. Davis, A.S.M. International., Handbook of materials for medical devices, ASM International, Materials Park, OH, 2006.

[2] M. Geetha, A.K. Singh, R. Asokamani, A.K. Gogia, Ti based biomaterials, the ultimate choice for orthopaedic implants - A review, Prog. Mater. Sci. 54 (2009) 397–425. doi:10.1016/j.pmatsci.2008.06.004.

[3] B. D. Ratner, A. S. Hoffman, F.J. Schoen, Biomaterials Science, Third Edition: An Introduction to Materials in Medicine, Academic Press, 2013.

[4] J.J. Jacobs, R.M. Urban, J.L. Gilbert, Corrosion of metal orthopaedic implants, J. Bone Jt. Surg. Am. 80 (1998) 268–282.

[5] K. Yang, Y. Ren, Nickel-free austenitic stainless steels for medical applications, Sci. Technol. Adv. Mater. 11 (2010) 014105. doi:10.1088/1468-6996/11/1/014105.

[6] Y. Okazaki, E. Gotoh, Comparison of metal release from various metallic biomaterials in vitro, Biomaterials. 26 (2005) 11–21. doi:10.1016/J.BIOMATERIALS.2004.02.005.

[7] N.B. Hakiki, S. Boudin, B. Rondot, M. Da Cunha Belo, The electronic structure of passive films formed on stainless steels, Corros. Sci. 37 (1995) 1809–1822. doi:10.1016/0010-938X(95)00084-W.

[8] N.E. Hakiki, Semiconducting Properties of Passive Films Formed on Stainless Steels, J. Electrochem. Soc. 145 (1998) 3821–3829. doi:10.1149/1.1838880.

[9] R. Singh, N.B. Dahotre, Corrosion degradation and prevention by surface modification of biometallic materials, J. Mater. Sci. Mater. Med. 18 (2007) 725–751. doi:10.1007/s10856-006-0016-y.

[10] J. Jagielski, A. Piatkowska, P. Aubert, L. Thomé, A. Turos, A. Abdul Kader, Ion implantation for surface modification of biomaterials, Surf. Coatings Technol. 200 (2006) 6355–6361. doi:10.1016/j.surfcoat.2005.11.005.

[11] V. Muthukumaran, V. Selladurai, S. Nandhakumar, M. Senthilkumar, Experimental investigation on corrosion and hardness of ion implanted AISI 316L stainless steel, Mater. Des. 31 (2010) 2813–2817. doi:10.1016/j.matdes.2010.01.007.

[12] C. Anandan, V.K. William Grips, V. Ezhil Selvi, K.S. Rajam, Electrochemical studies of stainless steel implanted with nitrogen and oxygen by plasma immersion ion implantation, Surf. Coatings Technol. 201 (2007) 7873–7879. doi:10.1016/j.surfcoat.2007.03.034.

[13] L. Wang, X. Zhao, M.H. Ding, H. Zheng, H.S. Zhang, B. Zhang, X.Q. Li, G.Y. Wu,

Surface modification of biomedical AISI 316L stainless steel with zirconium carbonitride coatings, Appl. Surf. Sci. 340 (2015) 113–119. doi:10.1016/j.apsusc.2015.02.191.

[14] A. Sharifnabi, M.H. Fathi, B. Eftekhari Yekta, M. Hossainalipour, The structural and bio-corrosion barrier performance of Mg-substituted fluorapatite coating on 316L stainless steel human body implant, Appl. Surf. Sci. 288 (2014) 331–340. doi:10.1016/j.apsusc.2013.10.029.

[15] S. Pourhashem, A. Afshar, Double layer bioglass-silica coatings on 316L stainless steel by sol-gel method, Ceram. Int. 40 (2014) 993–1000. doi:10.1016/j.ceramint.2013.06.096.

[16] B. Al-Mangour, R. Mongrain, E. Irissou, S. Yue, Improving the strength and corrosion resistance of 316L stainless steel for biomedical applications using cold spray, Surf. Coatings Technol. 216 (2013) 297–307. doi:10.1016/j.surfcoat.2012.11.061.

[17] S. Habibzadeh, L. Li, D. Shum-Tim, E.C. Davis, S. Omanovic, Electrochemical polishing as a 316L stainless steel surface treatment method: Towards the improvement of biocompatibility, Corros. Sci. 87 (2014) 89–100. doi:10.1016/j.corsci.2014.06.010.

[18] A. Latifi, M. Imani, M.T. Khorasani, M.D. Joupari, Electrochemical and chemical methods for improving surface characteristics of 316L stainless steel for biomedical applications, Surf. Coatings Technol. 221 (2013) 1–12. doi:10.1016/j.surfcoat.2013.01.020.

[19] Z. ur Rahman, K.M. Deen, L. Cano, W. Haider, The effects of parametric changes in electropolishing process on surface properties of 316L stainless steel, Appl. Surf. Sci. 410 (2017) 432–444. doi:10.1016/j.apsusc.2017.03.081.

[20] M. Vuković, The formation and growth of hydrous oxide film on stainless steel in alkaline solution by potential cycling, Corros. Sci. 37 (1995) 111–120. doi:10.1016/0010-938X(94)00119-Q.

[21] Z. Bou-Saleh, A. Shahryari, S. Omanovic, Enhancement of corrosion resistance of a biomedical grade 316LVM stainless steel by potentiodynamic cyclic polarization, Thin Solid Films. 515 (2007) 4727–4737. doi:10.1016/j.tsf.2006.11.054.

[22] A. Shahryari, S. Omanovic, J.A. Szpunar, Electrochemical formation of highly pitting resistant passive films on a biomedical grade 316LVM stainless steel surface, Mater. Sci. Eng. C. 28 (2008) 94–106. doi:10.1016/j.msec.2007.09.002.

[23] P.M. Samim, A. Fattah-Alhosseini, Enhancing the electrochemical behavior of aisi 304 stainless steel by cyclic potentiodynamic passivation (CPP) method, Anal. Bioanal. Electrochem. 8 (2016) 717–731.

[24] S. Vafaeian, A. Fattah-Alhosseini, M.K. Keshavarz, Y. Mazaheri, The influence of cyclic

voltammetry passivation on the electrochemical behavior of fine and coarse-grained AISI 430 ferritic stainless steel in an alkaline solution, J. Alloys Compd. 677 (2016) 42–51. doi:10.1016/j.jallcom.2016.03.222.

[25] G.E. Badea, D. Ionita, P. Cret, Corrosion and passivation of the 304 stainless steel in formic acid solutions, Mater. Corros. 65 (2014) 1103–1110. doi:10.1002/maco.201307491.

[26] K.S. Raja, D.A. Jones, Effects of dissolved oxygen on passive behavior of stainless alloys, Corros. Sci. 48 (2006) 1623–1638. doi:10.1016/J.CORSCI.2005.05.048.

[27] Z. Feng, X. Cheng, C. Dong, L. Xu, X. Li, Effects of dissolved oxygen on electrochemical and semiconductor properties of 316L stainless steel, J. Nucl. Mater. 407 (2010) 171–177. doi:10.1016/j.jnucmat.2010.10.010.

[28] J.J. Kim, Y.M. Young, Study on the passive film of type 316 stainless steel, Int. J. Electrochem. Sci. 8 (2013) 11847–11859. doi:10.1117/12.2084776.

[29] I. Gurappa, Characterization of different materials for corrosion resistance under simulated body fluid conditions, Mater. Charact. 49 (2002) 73–79. doi:10.1016/S1044-5803(02)00320-0.

[30] M. Sivakumar, K.S. Kumar Dhanadurai, S. Rajeswari, V. Thulasiraman, Failures in stainless steel orthopaedic implant devices: A survey, J. Mater. Sci. Lett. 14 (1995) 351–354. doi:10.1007/BF00592147.

[31] A. Muñoz, M. Costa, Elucidating the mechanisms of nickel compound uptake: A review of particulate and nano-nickel endocytosis and toxicity, Toxicol. Appl. Pharmacol. 260 (2012) 1–16. doi:10.1016/j.taap.2011.12.014.

[32] M. Niinomi, M. Nakai, J. Hieda, Development of new metallic alloys for biomedical applications, Acta Biomater. 8 (2012) 3888–3903. doi:10.1016/j.actbio.2012.06.037.

[33] T. Hu, C. Yang, S. Lin, Q. Yu, G. Wang, Biodegradable stents for coronary artery disease treatment: Recent advances and future perspectives, Mater. Sci. Eng. C. 91 (2018) 163–178. doi:10.1016/j.msec.2018.04.100.

[34] C.C. Shih, S.J. Lin, K.H. Chung, Y.L. Chen, Y.Y. Su, Increased corrosion resistance of stent materials by converting current surface film of polycrystalline oxide into amorphous oxide, J. Biomed. Mater. Res. 52 (2000) 323–332. doi:10.1002/1097-4636(200011)52:2<323::AID-JBM11>3.0.CO;2-Z.

[35] C.C. Shih, C.M. Shih, Y.Y. Su, L.H.J. Su, M.S. Chang, S.J. Lin, Effect of surface oxide properties on corrosion resistance of 316L stainless steel for biomedical applications, Corros. Sci. 46 (2004) 427–441. doi:10.1016/S0010-938X(03)00148-3.

[36] C.L. McBee, J. Kruger, Nature of passive films on iron-chromium alloys, Electrochim. Acta. 17 (1972) 1337–1341. doi:10.1016/0013-4686(72)80079-3.

[37] M.P. Ryan, R.C. Newman, G.E. Thompson, Atomically Resolved STM of Oxide Film Structures on Fe-Cr Alloys during Passivation in Sulfuric Acid Solution, J. Electrochem. Soc. 141 (1994) L164–L165. doi:10.1149/1.2059380.

[38] M.P. Ryan, R.C. Newman, G.E. Thompson, An STM Study of the Passive Film Formed on Iron in Borate Buffer Solution, J. Electrochem. Soc. 142 (1995) L177–L179. doi:10.1149/1.2050035.

[39] P. Marcus, Surface science approach of corrosion phenomena, Electrochim. Acta. 43 (1998) 109–118. doi:10.1016/S0013-4686(97)00239-9.

[40] D. Wallinder, J. Pan, C. Leygraf, A. Delblanc-Bauer, EIS and XPS study of surface modification of 316LVM stainless steel after passivation, Corros. Sci. 41 (1998) 275–289. doi:10.1016/S0010-938X(98)00122-X.

[41] H. Xu, L. Wang, D. Sun, H. Yu, The passive oxide films growth on 316L stainless steel in borate buffer solution measured by real-time spectroscopic ellipsometry, Appl. Surf. Sci. 351 (2015) 367–373. doi:10.1016/j.apsusc.2015.05.165.

[42] C.-O.A. Olsson, D. Landolt, Film Growth during Anodic Polarization in the Passive Region on 304 Stainless Steels with Cr, Mo, or W Additions Studied with EQCM and XPS, J. Electrochem. Soc. 148 (2001) B438–B449. doi:10.1149/1.1404969.

[43] G. Lorang, M.D.C. Belo, A.M.P. Simões, M.G.S. Ferreira, Chemical Composition of Passive Films on AISI 304 Stainless Steel, J. Electrochem. Soc. 141 (1994) 3347–3356. doi:10.1149/1.2059338.

[44] M.F. Montemor, M.G.S. Ferreira, N.E. Hakiki, M. Da Cunha Belo, Chemical composition and electronic structure of the oxide films formed on 316L stainless steel and nickel based alloys in high temperature aqueous environments, Corros. Sci. 42 (2000) 1635–1650. doi:10.1016/S0010-938X(00)00012-3.

[45] T. Hong, T. Ogushi, M. Nagumo, The effect of chromium enrichment in the film formed by surface treatments on the corrosion resistance of type 430 stainless steel, Corros. Sci. 38 (1996) 881–888. doi:10.1016/0010-938X(96)00174-6.

[46] R. Kirchheim, B. Heine, H. Fischmeister, S. Hofmann, H. Knote, U. Stolz, The passivity of iron-chromium alloys, Corros. Sci. 29 (1989) 899–917. doi:10.1016/0010-938X(89)90060-7.

[47] S. Ningshen, U. Kamachi Mudali, V.K. Mittal, H.S. Khatak, Semiconducting and passive film properties of nitrogen-containing type 316LN stainless steels, Corros. Sci. 49 (2007)

481–496. doi:10.1016/j.corsci.2006.05.041.

[48] R.A. Antunes, M.C.L. De Oliveira, I. Costa, Study of the correlation between corrosion resistance and semi-conducting properties of the passive film of AISI 316L stainless steel in physiological solution, Mater. Corros. 63 (2012) 586–592. doi:10.1002/maco.201006052.

[49] A.M.P. Simões, M.G.S. Ferreira, B. Rondot, M. da C. Belo, Study of Passive Films Formed on AISI 304 Stainless Steel by Impedance Measurements and Photoelectrochemistry, J. Electrochem. Soc. 137 (1990) 82–87. doi:10.1149/1.2086444.

[50] J. Keir, Experiments and observations on the dissolution of metals in acids, and their precipitations; with an account of a new compound acid menstruum, useful in some technical operations of parting metals, Philos. Trans. R. Soc. London. 80 (1790) 359–384. doi:10.1098/rstl.1790.0024.

[51] D.D. Macdonald, Passivity–the key to our metals-based civilization, Pure Appl. Chem. 71 (1999) 951–978. doi:10.1351/pac199971060951.

[52] E.J.W. Verwey, Electrolytic conduction of a solid insulator at high fields The formation of the anodic oxide film on aluminium, Physica. 2 (1935) 1059–1063. doi:10.1016/S0031-8914(35)90193-8.

[53] K.J. Vetter, F. Gorn, Kinetics of layer formation and corrosion processes of passive iron in acid solutions, Electrochim. Acta. 18 (1973) 321–326. doi:10.1016/0013-4686(73)80036-2.

[54] N. Sato, An overview on the passivity of metals, Corros. Sci. 31 (1990) 1–19. doi:10.1016/0010-938X(90)90086-K.

[55] B. Aksakal, Ö.S. Yildirim, H. Gul, Metallurgical failure analysis of various implant materials used in orthopedic applications, J. Fail. Anal. Prev. 4 (2004) 17–23. doi:10.1361/15477020419794.

[56] K.L. Wapner, Implications of metallic corrosion in total knee arthroplasty, Clin. Orthop. Relat. Res. (1991) 12–20. doi:10.1097/00003086-199110000-00004.

[57] D.B. McGregor, R.A. Baan, C. Partensky, J.M. Rice, J.D. Wilbourn, Evaluation of the carcinogenic risks to humans associated with surgical implants and other foreign bodies - A report of an IARC Monographs Programme Meeting, in: Eur. J. Cancer, Pergamon, 2000: pp. 307–313. doi:10.1016/S0959-8049(99)00312-3.

[58] K.J. Bundy, Corrosion and other electrochemical aspects of biomaterials., Crit. Rev. Biomed. Eng. 22 (1994) 139–251.

[59] M. Sumita, T. Hanawa, I. Ohnishi, T. Yoneyama, 9.04 - Failure Processes in Biometallic Materials, in: Compr. Struct. Integr., 2003: pp. 131–167. doi:10.1016/B0-08-043749-4/09143-6.

[60] H. Boehni, Breakdown of passivity and localized corrosion processes, Langmuir. 3 (1987) 924–930. doi:10.1021/la00078a010.

[61] M. Sivakumar, U. Kamachi Mudali, S. Rajeswari, Investigation of failures in stainless steel orthopaedic implant devices: fatigue failure due to improper fixation of a compression bone plate, J. Mater. Sci. Lett. 13 (1994) 142–145. doi:10.1007/BF00416827.

[62] T.M. Sridhar, U. Kamachi Mudali, M. Subbaiyan, Preparation and characterisation of electrophoretically deposited hydroxyapatite coatings on type 316L stainless steel, Corros. Sci. 45 (2003) 237–252. doi:10.1016/S0010-938X(02)00091-4.

[63] H. -H Strehblow, Nucleation and Repassivation of Corrosion Pits for Pitting on Iron and Nickel, Mater. Corros. 27 (1976) 792–799. doi:10.1002/maco.19760271106.

[64] T.P. Hoar, D.C. Mears, G.P. Rothwell, The relationships between anodic passivity, brightening and pitting, Corros. Sci. 5 (1965) 279–289. doi:10.1016/S0010-938X(65)90614-1.

[65] C.Y. Chao, L.F. Lin, D.D. Macdonald, A Point Defect Model for Anodic Passive Films I. Film growth kinetics, J. Electrochem. Soc. 128 (1981) 1187–1194. doi:10.1149/1.2127591.

[66] L.F. Lin, C.Y. Chao, D.D. Macdonald, A Point Defect Model for Anodic Passive Films II . Chemical Breakdown and Pit Initiation, J. Electrochem. Soc. 128 (1981) 1194–1198. doi:10.1149/1.2127592.

[67] D.D. Macdonald, The Point Defect Model for the Passive State, J. Electrochem. Soc. 139 (1992) 3434–3449. doi:10.1149/1.2069096.

[68] N. Sato, A theory for breakdown of anodic oxide films on metals, Electrochim. Acta. 16 (1971) 1683–1692. doi:10.1016/0013-4686(71)85079-X.

[69] N. Sato, K. Kudo, T. Noda, The anodic oxide film on iron in neutral solution, Electrochim. Acta. 16 (1971) 1909–1921. doi:10.1016/0013-4686(71)85146-0.

[70] S. Haupt, H.H. Strehblow, Corrosion, layer formation, and oxide reduction of passive iron in alkaline solution: a combined electrochemical and surface analytical study, Langmuir. 3 (1987) 873–885. doi:10.1021/la00078a003.

[71] J.M. Kolotyrkin, Pitting Corrosion of Metals, CORROSION. 19 (1963) 261t–268t. doi:10.5006/0010-9312-19.8.261.

[72] T.P. Hoar, W.R. Jacob, Breakdown of passivity of stainless steel by halide ions [3], Nature. 216 (1967) 1299–1301. doi:10.1038/2161299a0.

[73] E. McCafferty, Introduction to corrosion science, Springer New York, New York, NY, 2010. doi:10.1007/978-1-4419-0455-3.

[74] C. Pallotta, N. De Cristofano, R.C. Salvarezza, A.J. Arvia, The influence of temperature and the role of chromium in the passive layer in relation to pitting corrosion of 316 stainless steel in NaCl solution, Electrochim. Acta. 31 (1986) 1265–1270. doi:10.1016/0013-4686(86)80146-3.

[75] M. Urretabizkaya, C.D. Pallotta, N. De Cristofaro, R.C. Salvarezza, A.J. Arvia, Changes in the composition of the passive layer and pitting corrosion of stainless steel in phosphate-borate buffer containing chloride ions, Electrochim. Acta. 33 (1988) 1645–1651. doi:10.1016/0013-4686(88)80237-8.

[76] L.L. Hench, Bioceramics: From Concept to Clinic, J. Am. Ceram. Soc. 74 (1991) 1487–1510. doi:10.1111/j.1151-2916.1991.tb07132.x.

[77] M.H. Fathi, M. Salehi, A. Saatchi, V. Mortazavi, S.B. Moosavi, In vitro corrosion behavior of bioceramic, metallic, and bioceramic-metallic coated stainless steel dental implants, Dent. Mater. 19 (2003) 188–198. doi:10.1016/S0109-5641(02)00029-5.

[78] D. Liu, K. Savino, M.Z. Yates, Coating of hydroxyapatite films on metal substrates by seeded hydrothermal deposition, Surf. Coatings Technol. 205 (2011) 3975–3986. doi:10.1016/j.surfcoat.2011.02.008.

[79] L. Sun, C.C. Berndt, K.A. Gross, A. Kucuk, Material fundamentals and clinical performance of plasma-sprayed hydroxyapatite coatings: A review, J. Biomed. Mater. Res. 58 (2001) 570–592. doi:10.1002/jbm.1056.

[80] C. García, S. Ceré, A. Durán, Bioactive coatings prepared by sol-gel on stainless steel 316L, in: J. Non. Cryst. Solids, North-Holland, 2004: pp. 218–224. doi:10.1016/j.jnoncrysol.2004.08.172.

[81] N. Eliaz, M. Eliyahu, Electrochemical processes of nucleation and growth of hydroxyapatite on titanium supported by real-time electrochemical atomic force microscopy, J. Biomed. Mater. Res. - Part A. 80 (2007) 621–634. doi:10.1002/jbm.a.30944.

[82] L.-F. Li, J.-P. Celis, Pickling of austenitic stainless steels: A review, Can. Metall. Q. 42 (2003) 365–376. doi:10.1179/cmq.2003.42.3.365.

[83] J.S. Noh, N.J. Laycock, W. Gao, D.B. Wells, Effects of nitric acid passivation on the pitting resistance of 316 stainless steel, Corros. Sci. 42 (2000) 2069–2084.

doi:10.1016/S0010-938X(00)00052-4.

[84] K. Prabakaran, S. Rajeswari, Electrochemical, SEM and XPS investigations on phosphoric acid treated surgical grade type 316L SS for biomedical applications, J. Appl. Electrochem. 39 (2009) 887–897. doi:10.1007/s10800-008-9738-5.

[85] K.B. Hensel, Electropolishing, Met. Finish. 97 (1999) 440–448. doi:10.1016/S0026-0576(00)83104-9.

[86] P.J. Núñez, E. García-Plaza, M. Hernando, R. Trujillo, Characterization of surface finish of electropolished stainless steel AISI 316L with varying electrolyte concentrations, in: Procedia Eng., Elsevier, 2013: pp. 771–778. doi:10.1016/j.proeng.2013.08.255.

[87] N.N. Khobragade, A. V Bansod, A.P. Patil, Effect of dissolved oxygen on the corrosion behavior of 304 SS in 0.1 N nitric acid containing chloride, Mater. Res. Express. 5 (2018) 046526. doi:10.1088/2053-1591/aab8de.

[88] J. Morales, P. Esparza, R. Salvarezza, S. Gonzalez, The pitting and crevice corrosion of 304 stainless steel in phosphate-borate buffer containing sodium chloride, Corros. Sci. 33 (1992) 1645–1651. doi:10.1016/0010-938X(92)90040-A.

[89] T.L.S.L. Wijesinghe, D.J. Blackwood, Characterisation of passive films on 300 series stainless steels, Appl. Surf. Sci. 253 (2006) 1006–1009. doi:10.1016/j.apsusc.2006.03.081.

[90] S. Omanovic, S.G. Roscoe, Electrochemical studies of the adsorption behavior of bovine serum albumin on stainless steel, Langmuir. 15 (1999) 8315–8321. doi:10.1021/la990474f.

[91] S. Karimi, T. Nickchi, A. Alfantazi, Effects of bovine serum albumin on the corrosion behaviour of AISI 316L, Co–28Cr–6Mo, and Ti–6Al–4V alloys in phosphate buffered saline solutions, Corros. Sci. 53 (2011) 3262–3272. doi:10.1016/J.CORSCI.2011.06.009.